Measurement of the properties of the Higgs Boson in 13 TeV ATLAS data in the H->4ℓ decay channel

Will Leight

November 29, 2016

The LHC in Run-2

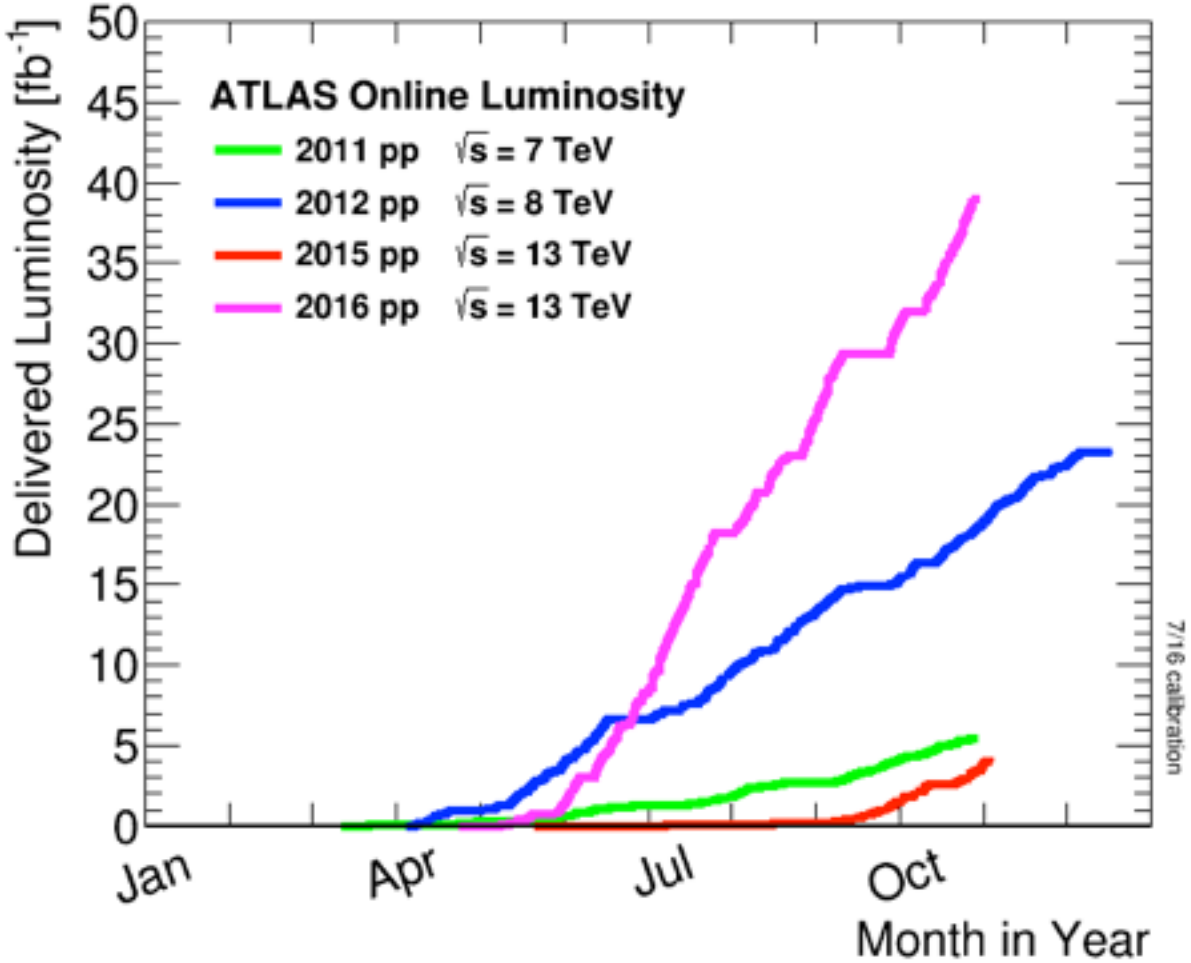

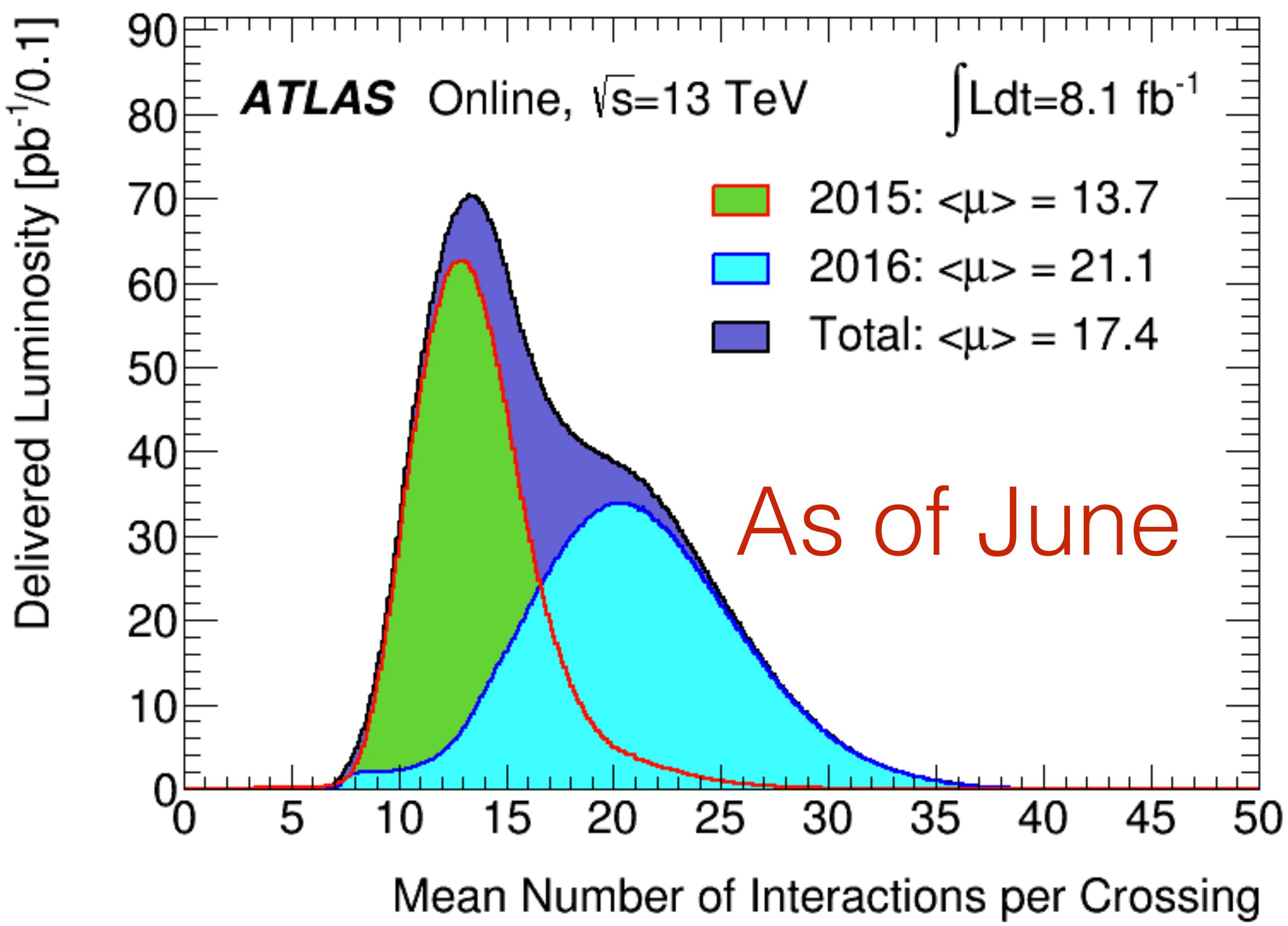

- Excellent performance by the LHC this year.
- The results shown here represent 13.3-14.8 fb^{-1} of data at 13 TeV recorded in 2015 and 2016.
  - Our sensitivity to the Higgs is now higher than it was in Run-1.

Higgs Boson Production

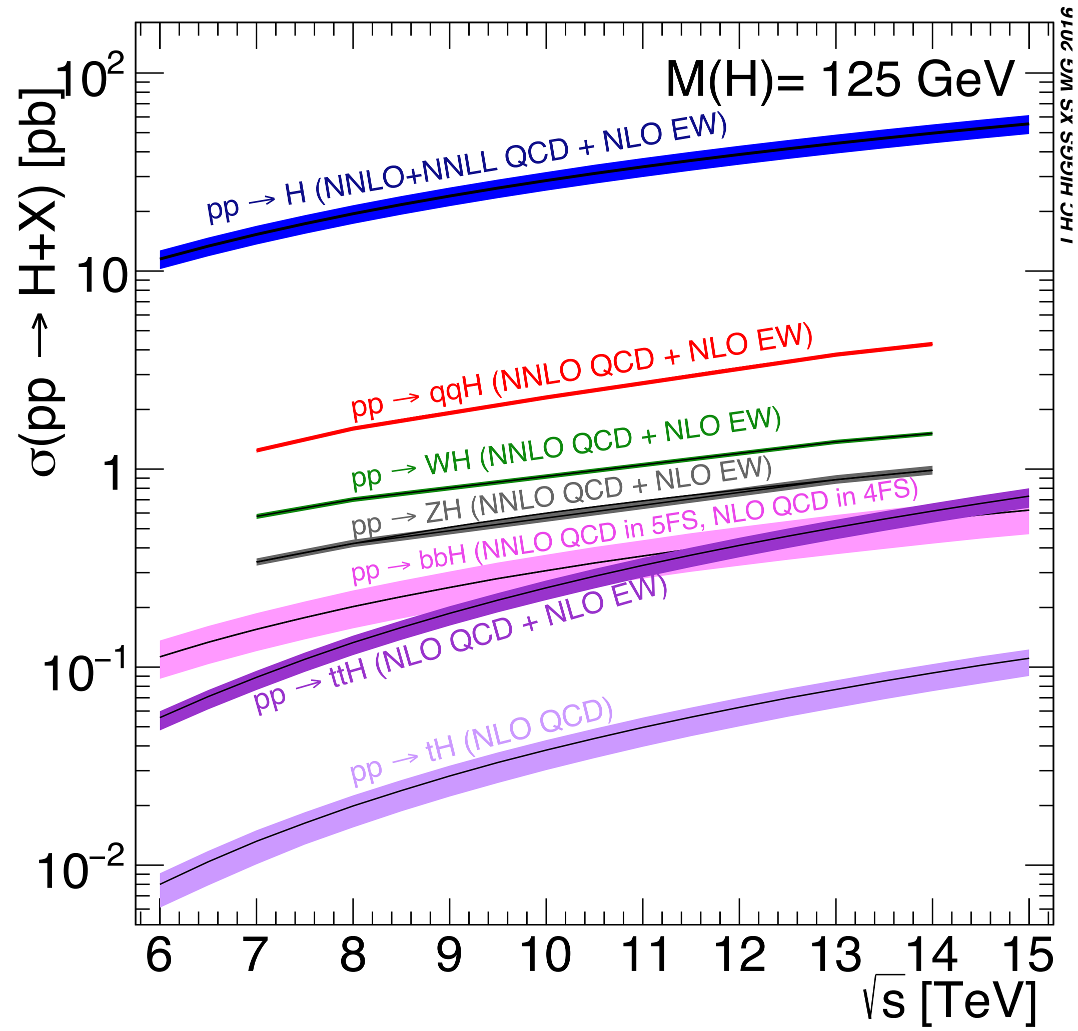

LHC Higgs XS WG

ggF	87.2%
VBF	6.8%
VH	4.1%
bbH/ttH/tH	1.9%

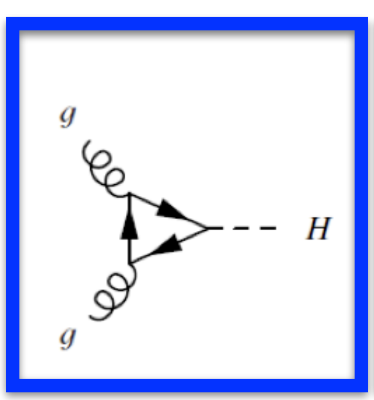

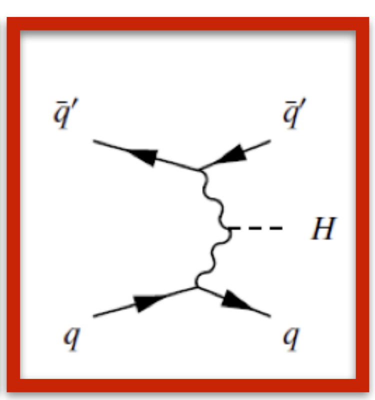

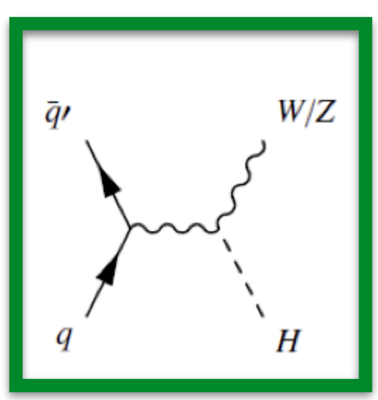

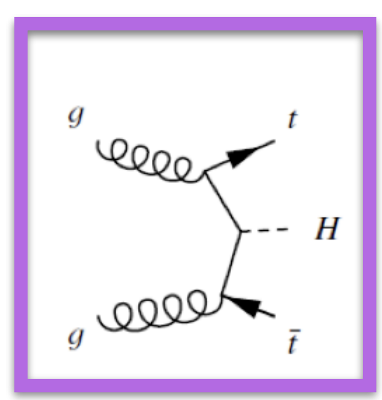

$\boldsymbol{\sigma}_{tot}$(13 TeV)~2$\boldsymbol{\sigma}_{tot}$(8 TeV)

arxiv 1101.0593

H->ZZ->4ℓ BR~.013%

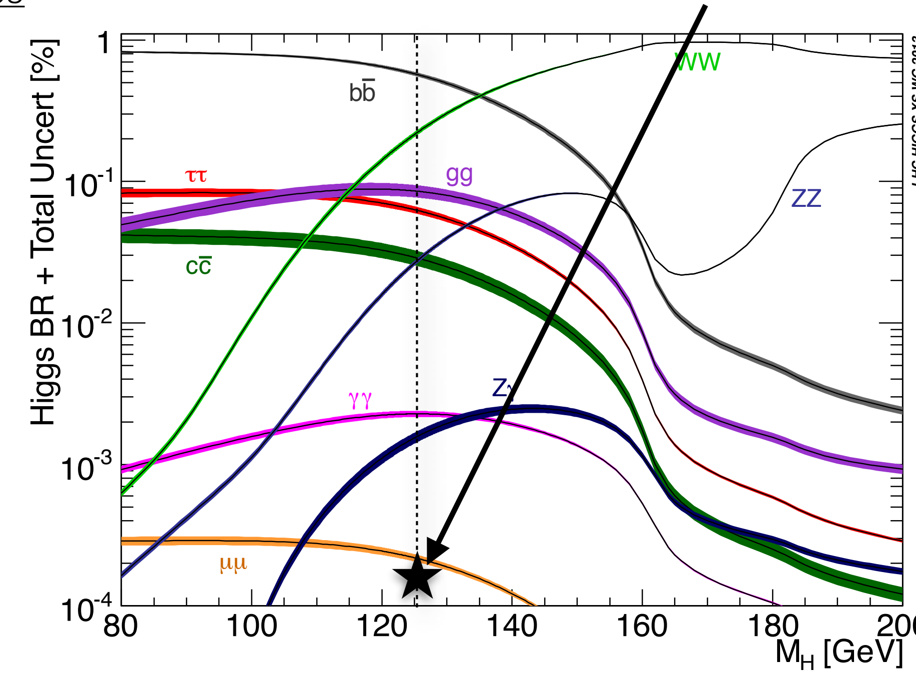

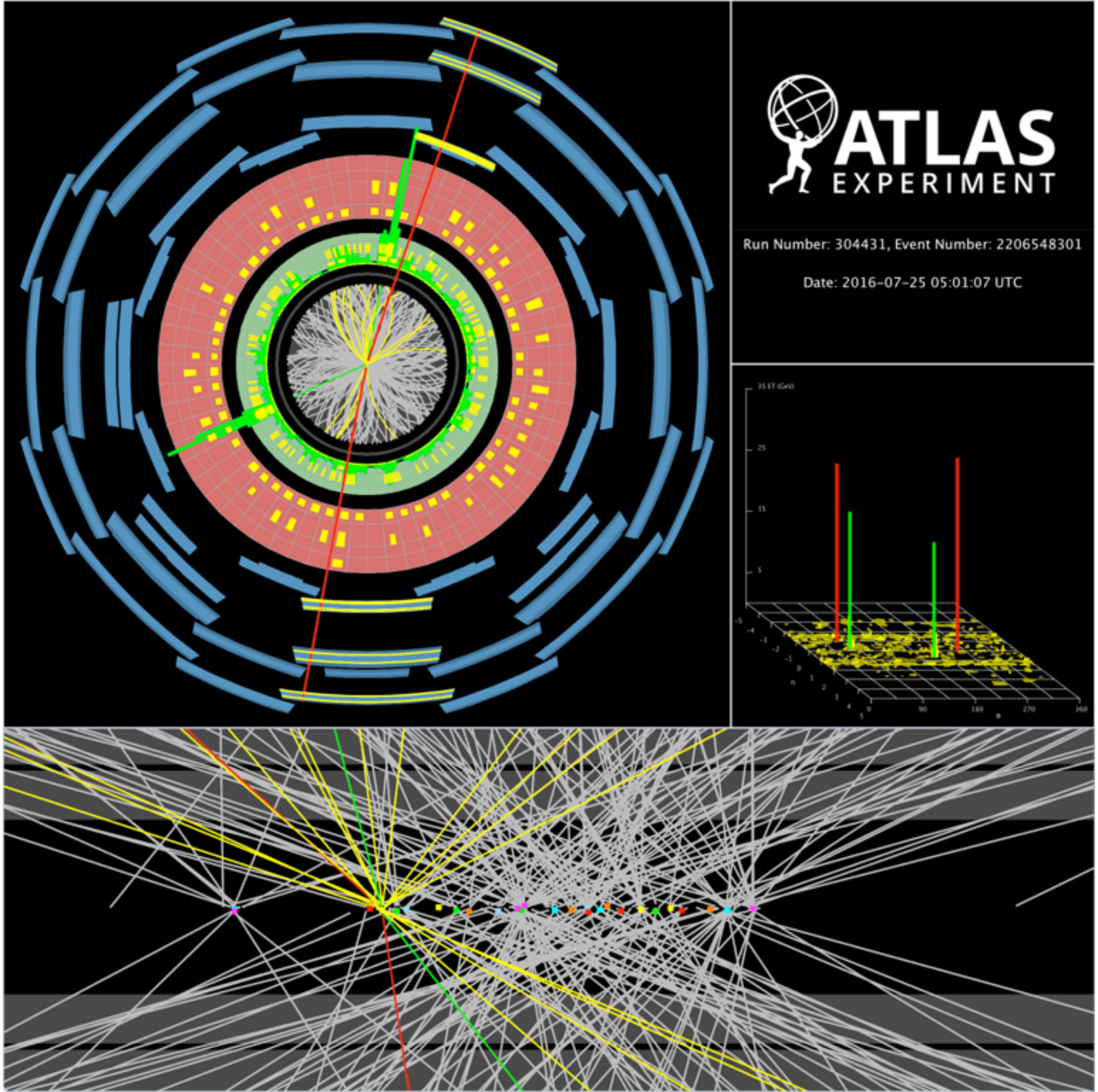
ATLAS
EXPERIMENT
Run Number: 304431, Event Number: 2206548301
Date: 2016-07-25 05:01:07 UTC

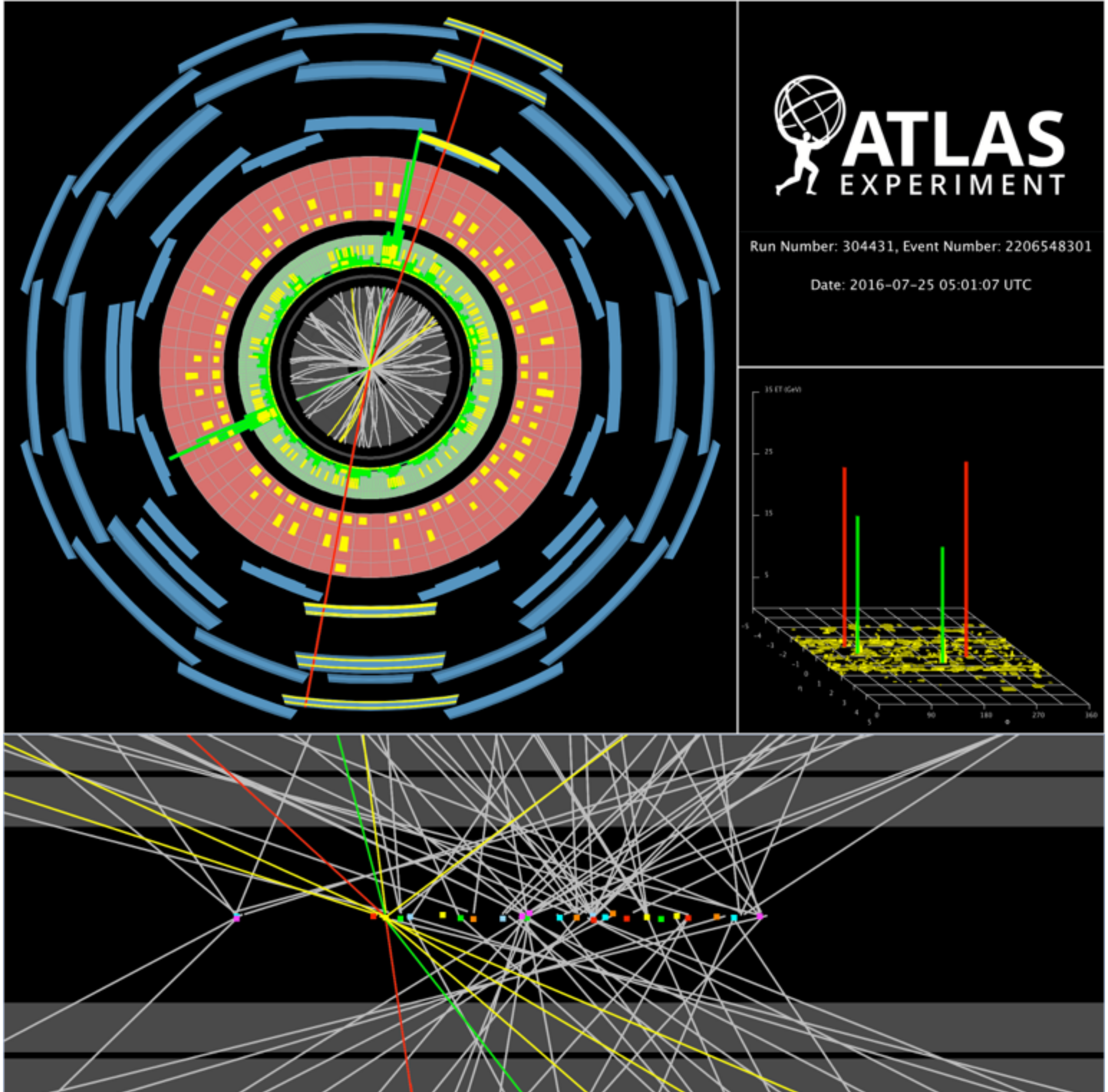
ATLAS
EXPERIMENT
Run Number: 304431, Event Number: 2206548301
Date: 2016-07-25 05:01:07 UTC

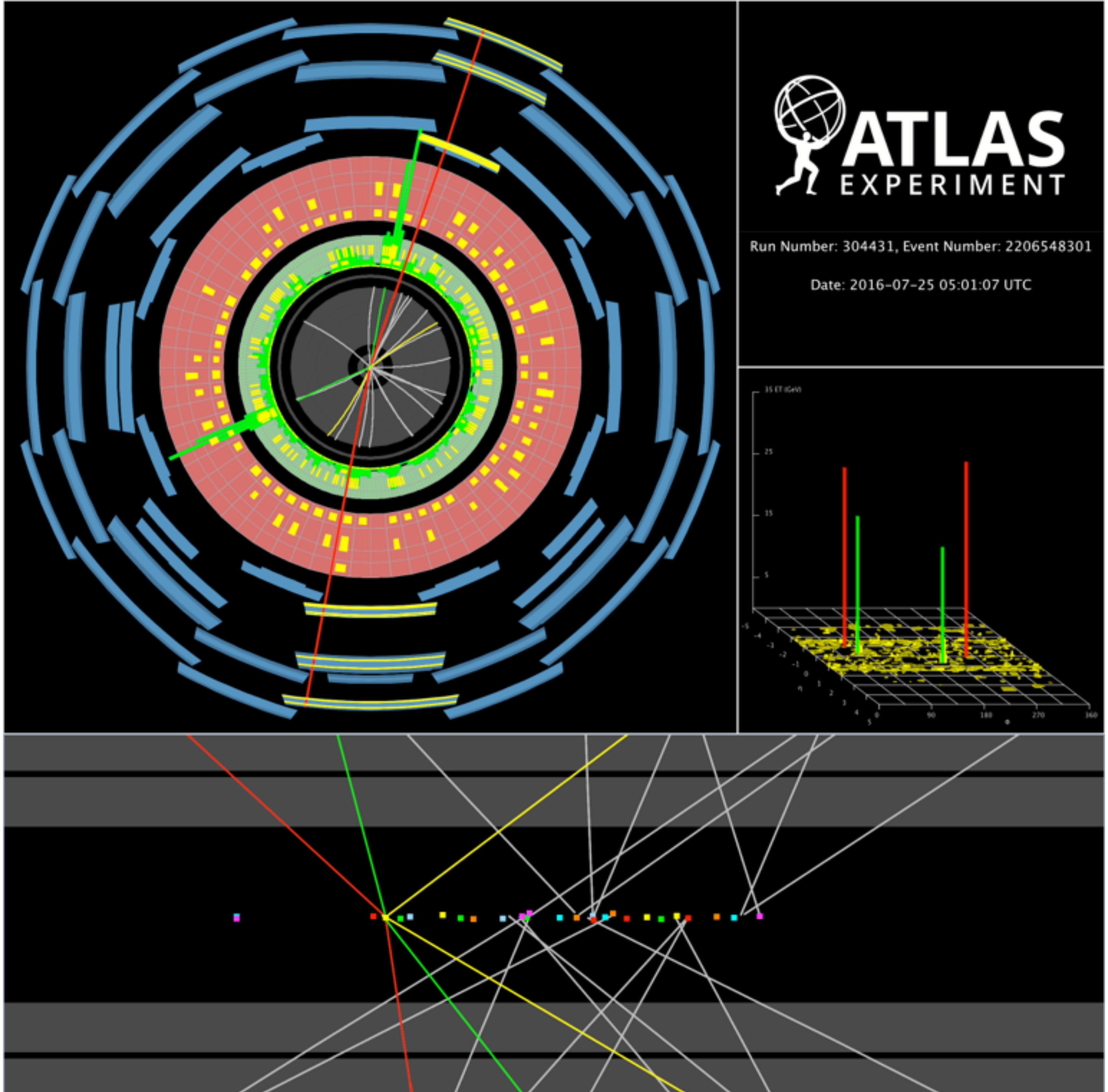
ATLAS
EXPERIMENT
Run Number: 304431, Event Number: 2206548301
Date: 2016-07-25 05:01:07 UTC

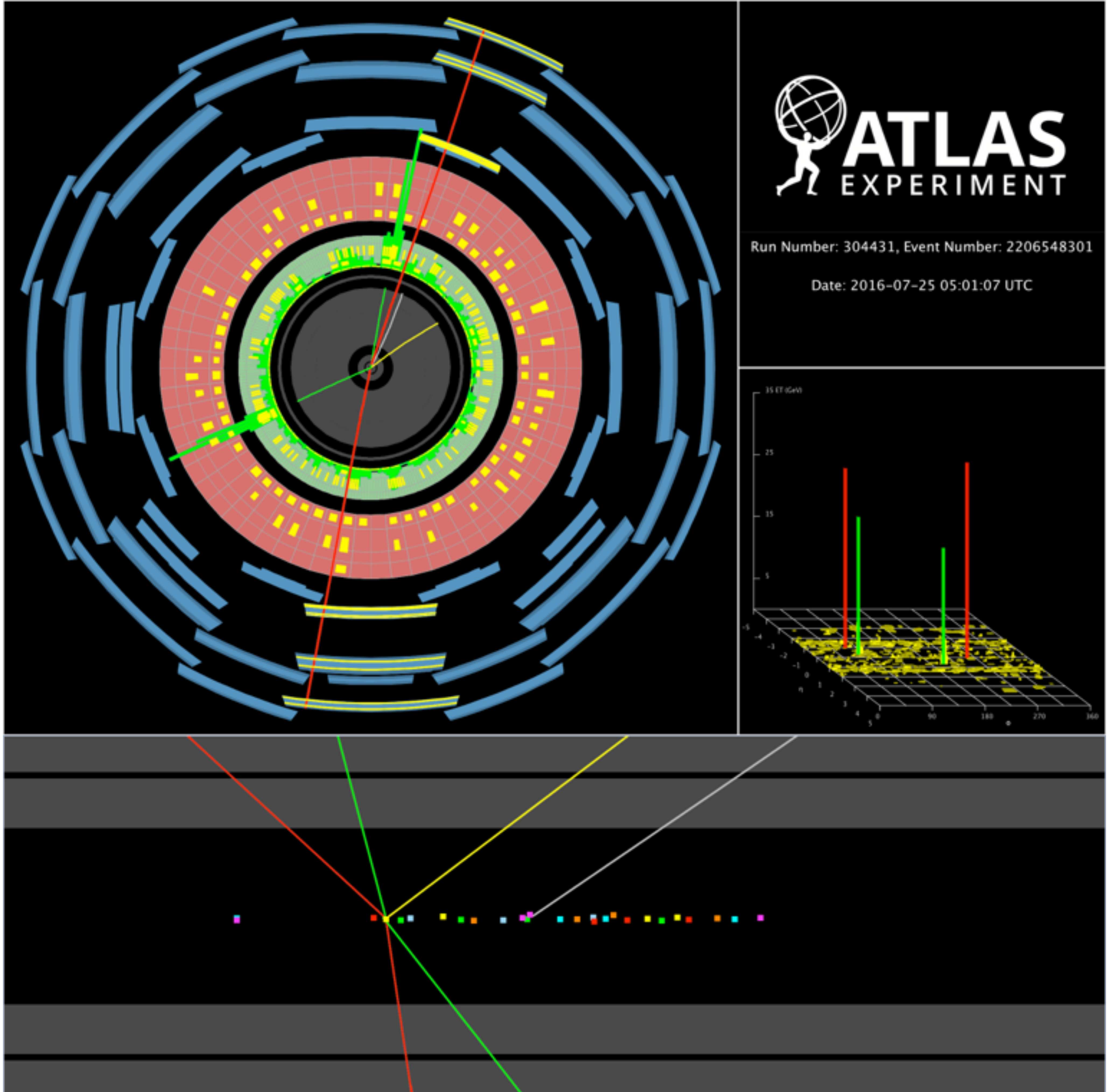
ATLAS
EXPERIMENT
Run Number: 304431, Event Number: 2206548301
Date: 2016-07-25 05:01:07 UTC

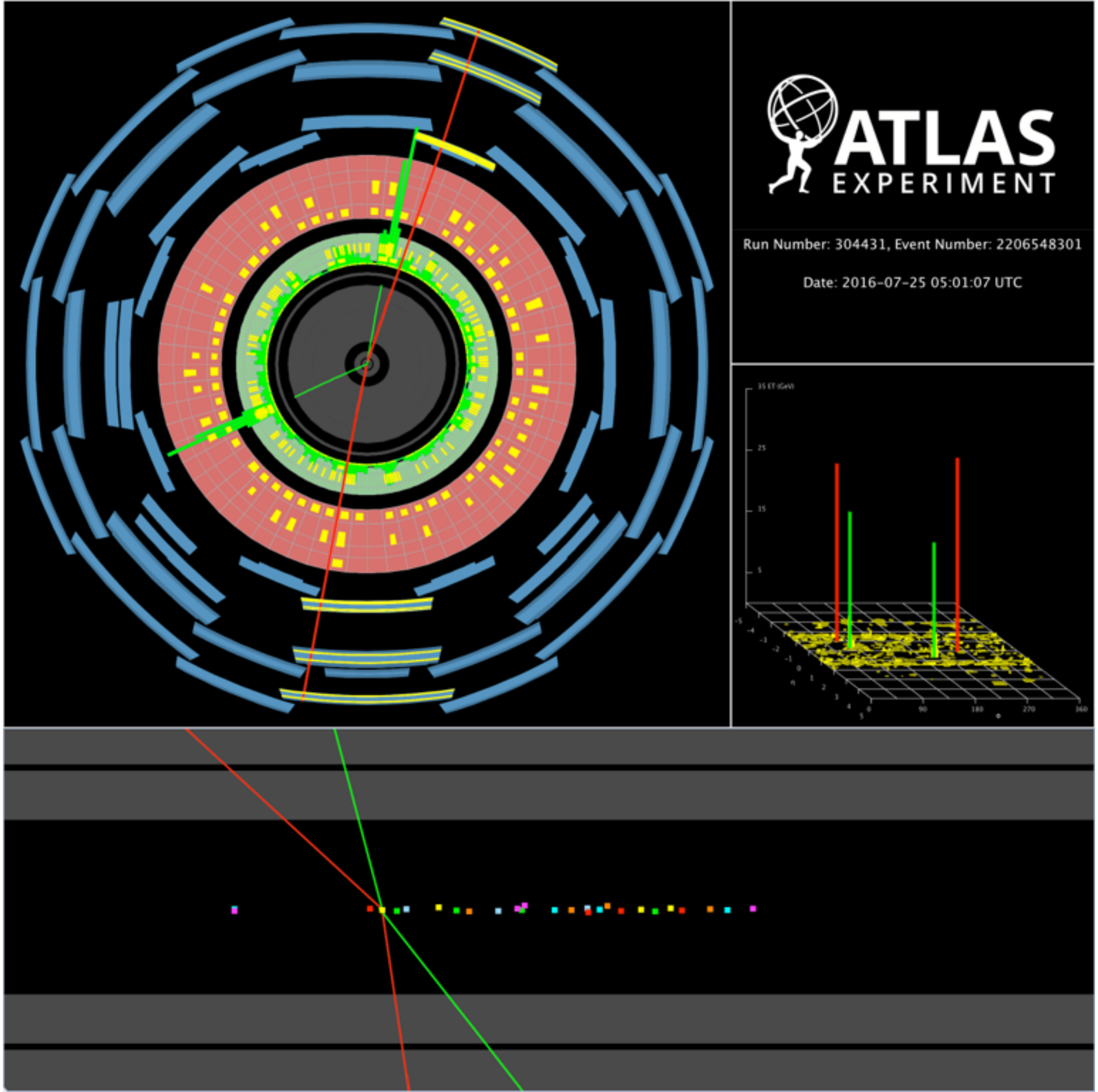
ATLAS
EXPERIMENT
Run Number: 304431, Event Number: 2206548301
Date: 2016-07-25 05:01:07 UTC

Recovering Efficiency With Loose Leptons

|η|<0.1 is not well instrumented -> fewer high-quality muons: use calo- and segment-tagged muons to recover efficiency.

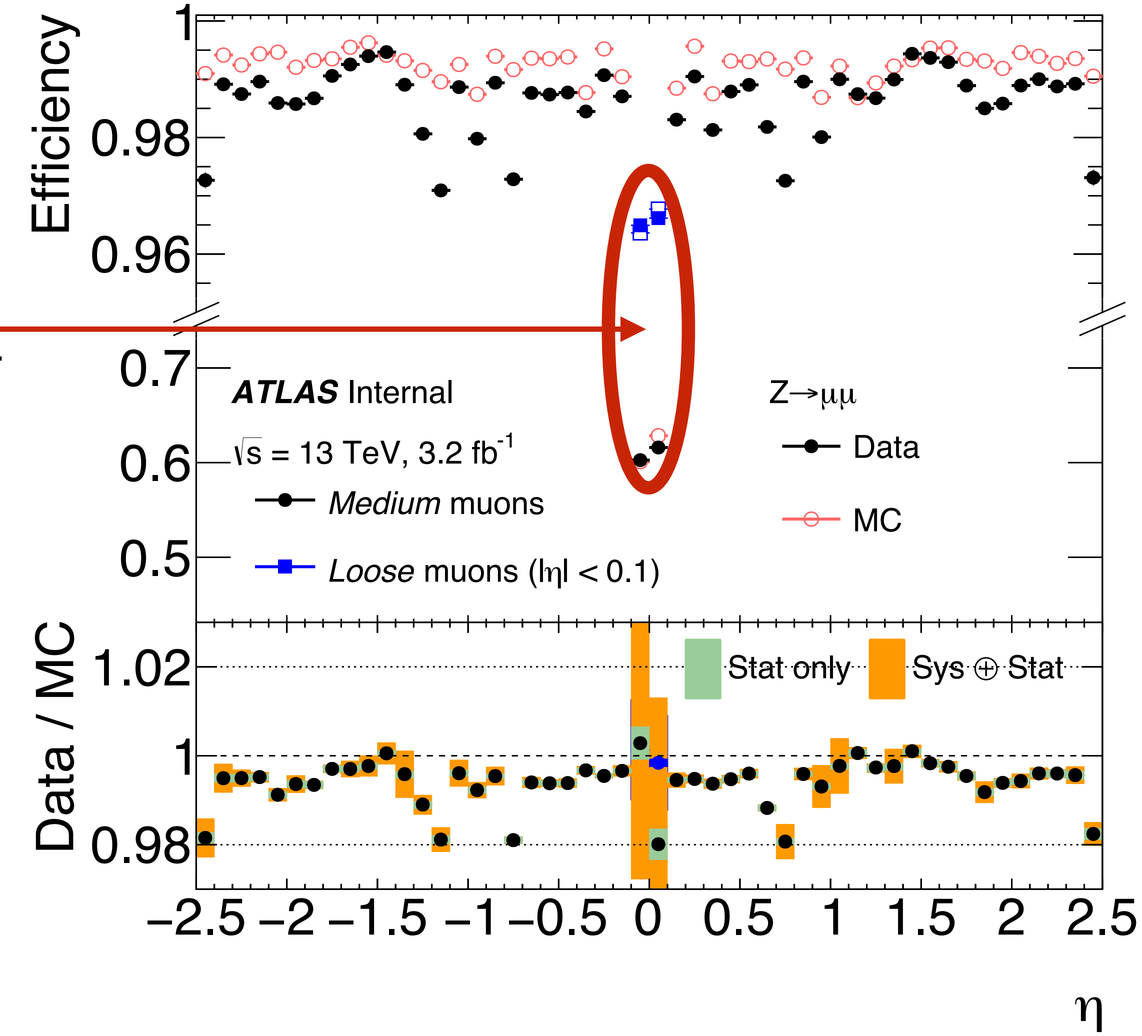

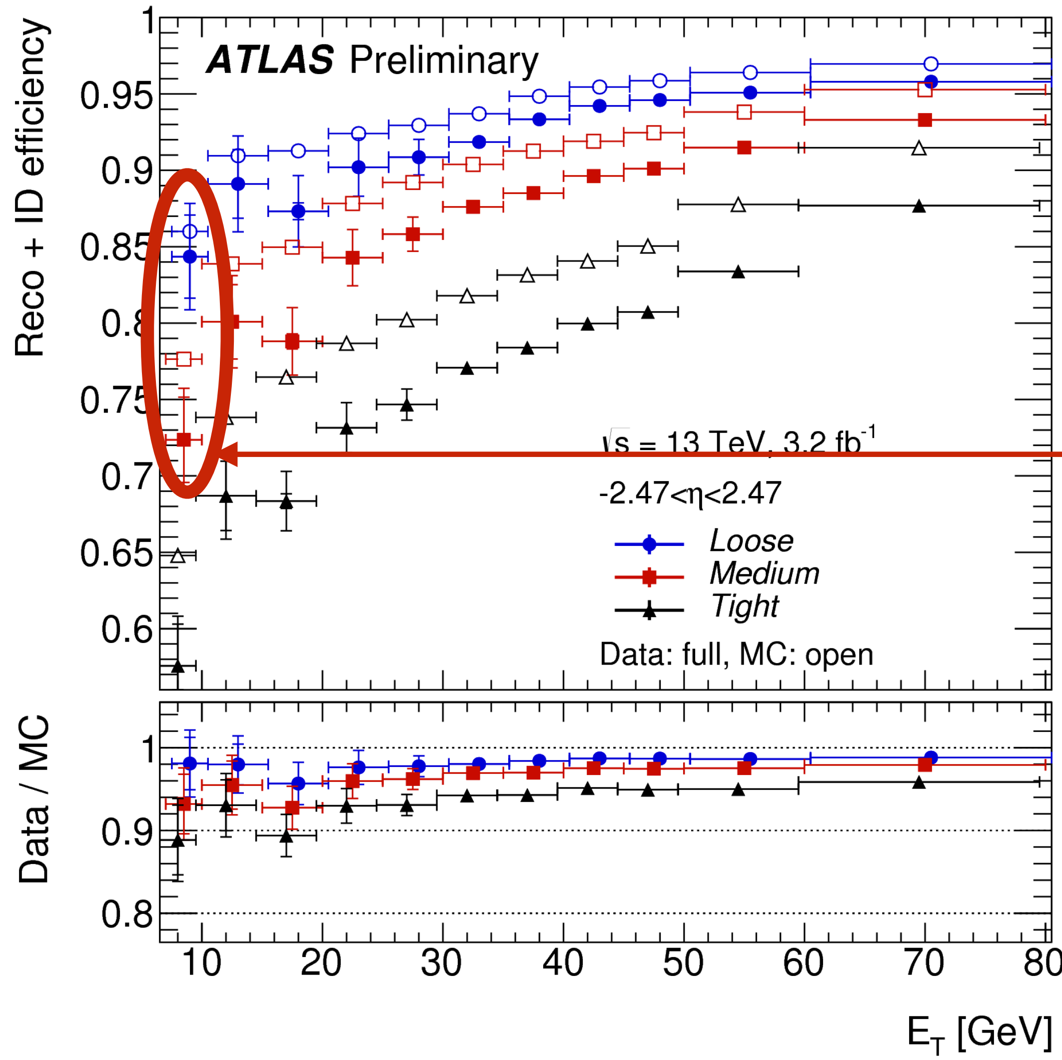

Loose electrons provide improved efficiency, especially at low p_T.

Event Selection

- Electron $E_T>7$, muon $p_T>5$ (excepting calo-tag muons)
  - Leading leptons in the quadruplet must have p_T of at least 20, 15, and 10 GeV
  - Isolation requirement to remove leptons from jets
  - d_0-significance requirement to remove leptons from heavy-flavor decays
  - Leading Z mass between $50<m_{\ell\ell}<106$ GeV, subleading $12<m_{\ell\ell}<115$ GeV
- Exploit properties of the event
  - 4ℓ vertexing constraint
  - m_{12} (+FSR photons) kinematically constrained to m_Z to improve the resolution.
- Improvements in Run-2
  - IBL provides superior rejection of electron backgrounds
  - Muon p_T cut from 6 to 5 GeV, +8% acceptance

The Higgs Peak

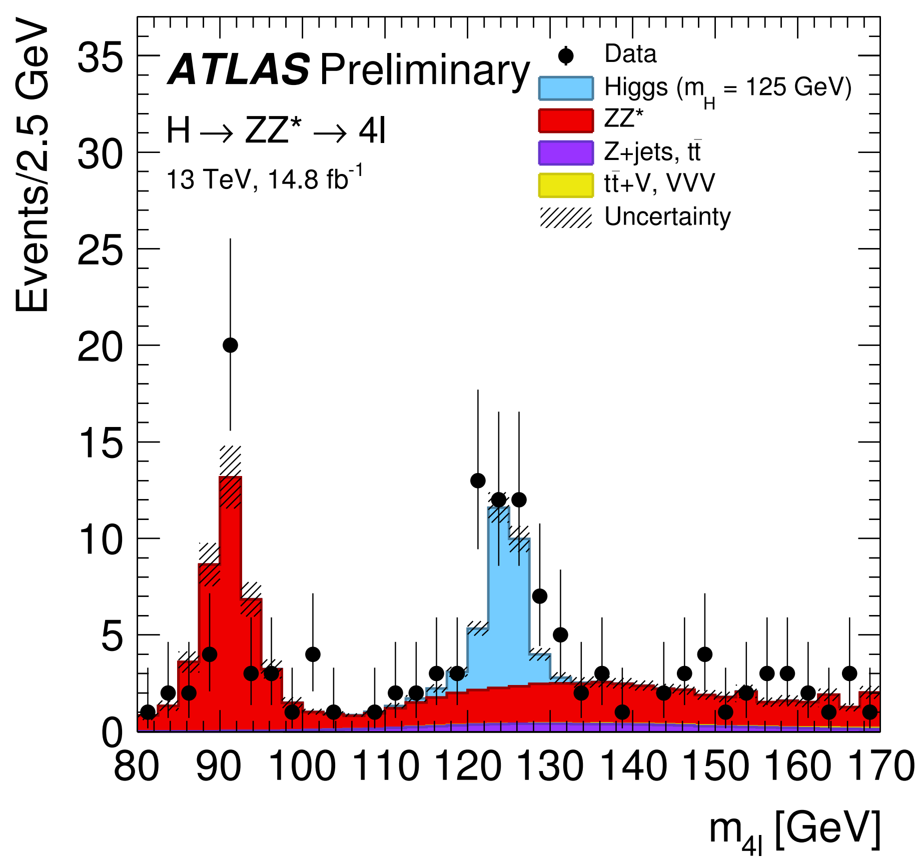

Final State	Signal full mass range	Signal	ZZ^*	Z + jets, $t\bar{t}$ ttV, VVV, WZ	S/B	Expected	Observed
4μ	8.8 ± 0.6	8.2 ± 0.6	3.11 ± 0.30	0.31 ± 0.04	2.4	11.6 ± 0.7	16
$2e2\mu$	6.1 ± 0.4	5.5 ± 0.4	2.19 ± 0.21	0.30 ± 0.04	2.2	8.0 ± 0.4	12
$2\mu 2e$	4.8 ± 0.4	4.4 ± 0.4	1.39 ± 0.16	0.47 ± 0.05	2.3	6.2 ± 0.4	10
$4e$	4.8 ± 0.5	4.2 ± 0.4	1.46 ± 0.18	0.46 ± 0.05	2.2	6.1 ± 0.4	6
Total	24.5 ± 1.8	22.3 ± 1.6	8.2 ± 0.8	1.54 ± 0.18	2.3	32.0 ± 1.8	44

ATLAS-CONF-2016-079

Background Estimates

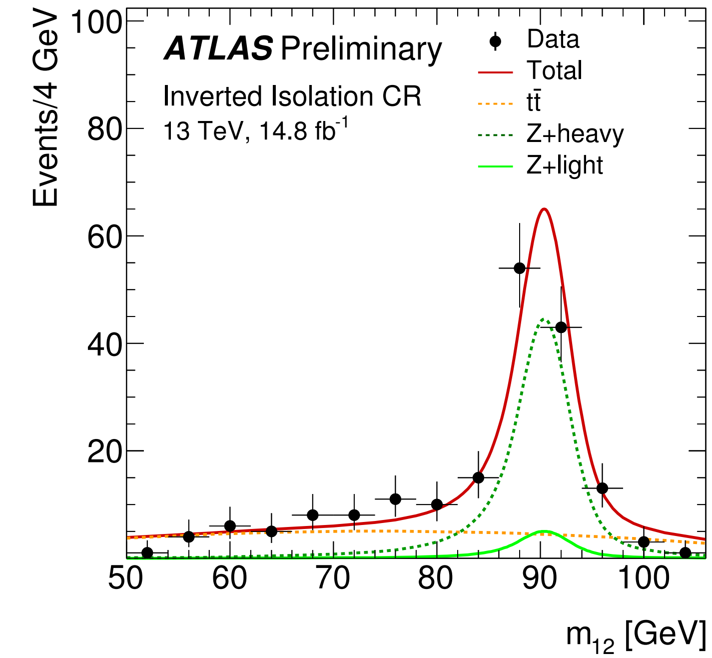

- Main background is ZZ* production, taken from simulation.
  - qq->ZZ simulated at NLO with POWHEG, QCD and EW corrections as a function of m_{ZZ}.
  - gg->ZZ simulated at LO with gg2VV, with a k-factor applied for higher-order QCD effects

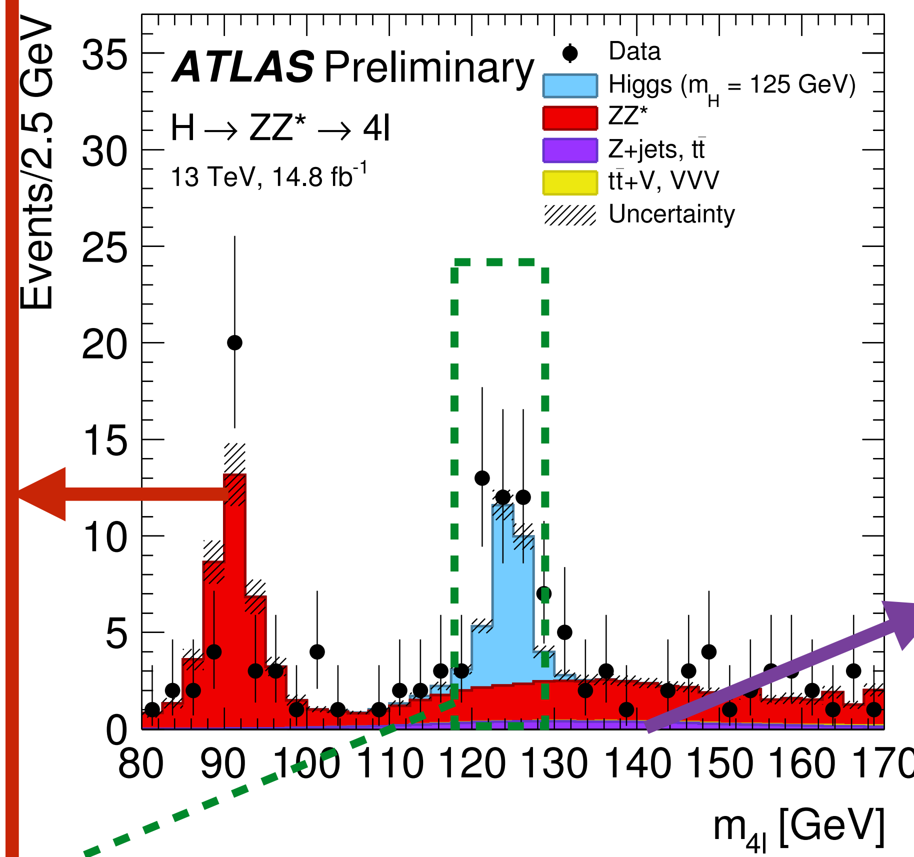

Reducible background from Z+jets and tt estimated using data-driven methods

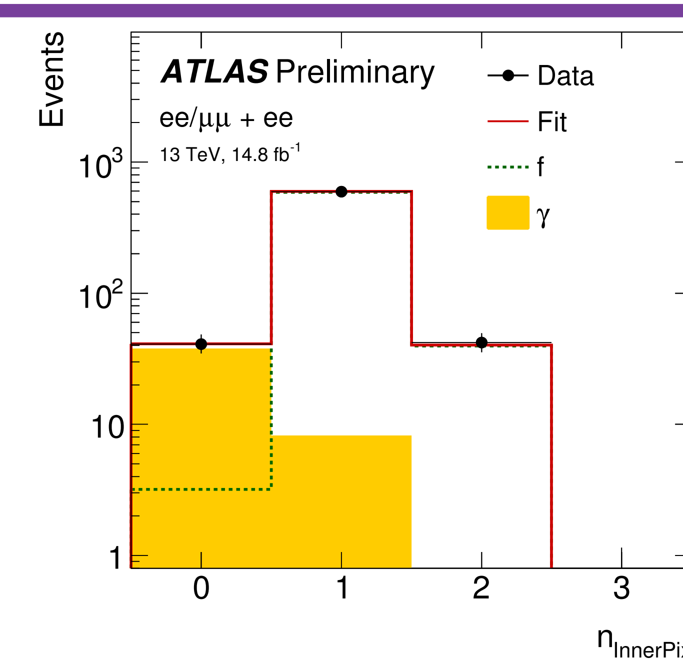

Final State	Signal full mass range	Signal	ZZ^*	$Z+\text{jets}, t\bar{t}$ $t\bar{t}V, VVV, WZ$	S/B	Expected	Observed
4μ	8.8 ± 0.6	8.2 ± 0.6	3.11 ± 0.30	0.31 ± 0.04	2.4	11.6 ± 0.7	16
$2e2\mu$	6.1 ± 0.4	5.5 ± 0.4	2.19 ± 0.21	0.30 ± 0.04	2.2	8.0 ± 0.4	12
$2\mu 2e$	4.8 ± 0.4	4.4 ± 0.4	1.39 ± 0.16	0.47 ± 0.05	2.3	6.2 ± 0.4	10
$4e$	4.8 ± 0.5	4.2 ± 0.4	1.46 ± 0.18	0.46 ± 0.05	2.2	6.1 ± 0.4	6
Total	24.5 ± 1.8	22.3 ± 1.6	8.2 ± 0.8	1.54 ± 0.18	2.3	32.0 ± 1.8	44

Fiducial Cross-Section

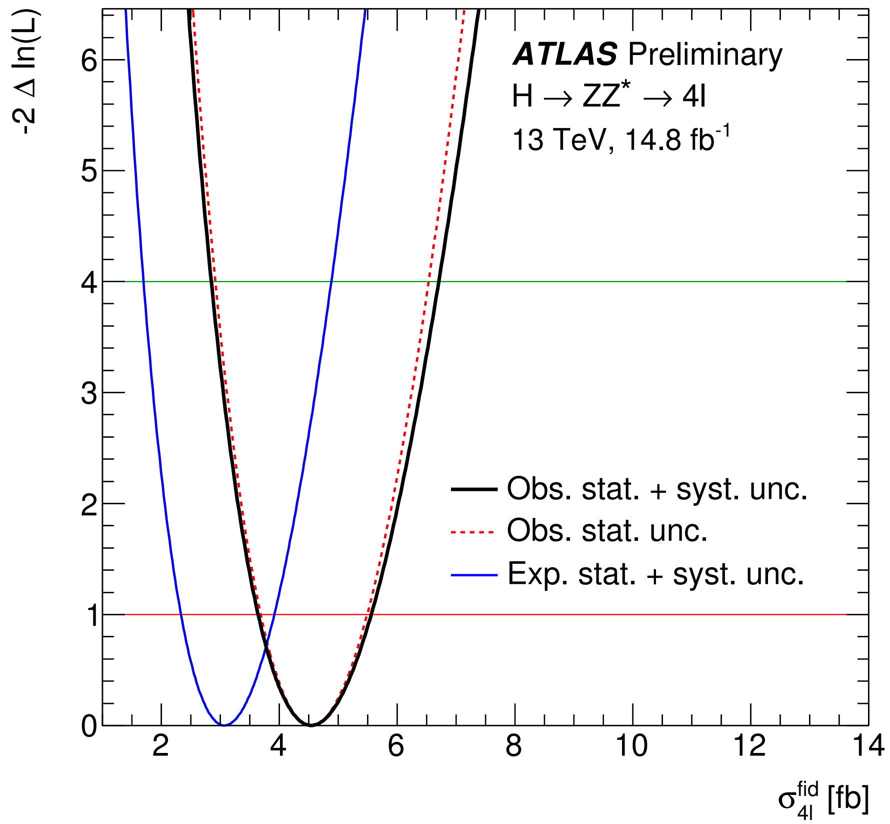

Final state	measured σ_{fid} [fb]	$\sigma_{\text{fid,SM}}$ [fb]
4μ	$1.28\,^{+0.48}_{-0.40}$	$0.93\,^{+0.06}_{-0.08}$
$4e$	$0.81\,^{+0.51}_{-0.38}$	$0.73\,^{+0.05}_{-0.06}$
$2\mu 2e$	$1.29\,^{+0.58}_{-0.46}$	$0.67\,^{+0.04}_{-0.04}$
$2e2\mu$	$1.10\,^{+0.49}_{-0.40}$	$0.76\,^{+0.05}_{-0.06}$

$$\boxed{\begin{aligned}\sigma_{\text{tot}} &= 81^{+18}_{-16}\ \text{pb}\\ \sigma_{\text{tot,SM}} &= 55.5^{+3.8}_{-4.4}\ \text{pb}\end{aligned}}$$

Uncertainties are still statistically dominated.
Compatible with SM at 1.6 σ.

- Fiducial cross-section is independent of assumptions about acceptance factors or branching ratios
  - Reduces model dependence
  - Only need to correct for detector efficiencies and resolution

$$\sigma^{fid}_{channel} = \frac{N_s}{\mathcal{C}.\mathcal{L}_{int}}$$

- Fiducial cross-section is obtained from a likelihood fit to the $m_{4\ell}$ distribution for $115 < m_{4\ell} < 130$ GeV.
  - Total cross-section is then obtained assuming SM BR and acceptance.

Cross-sections by Production Mode

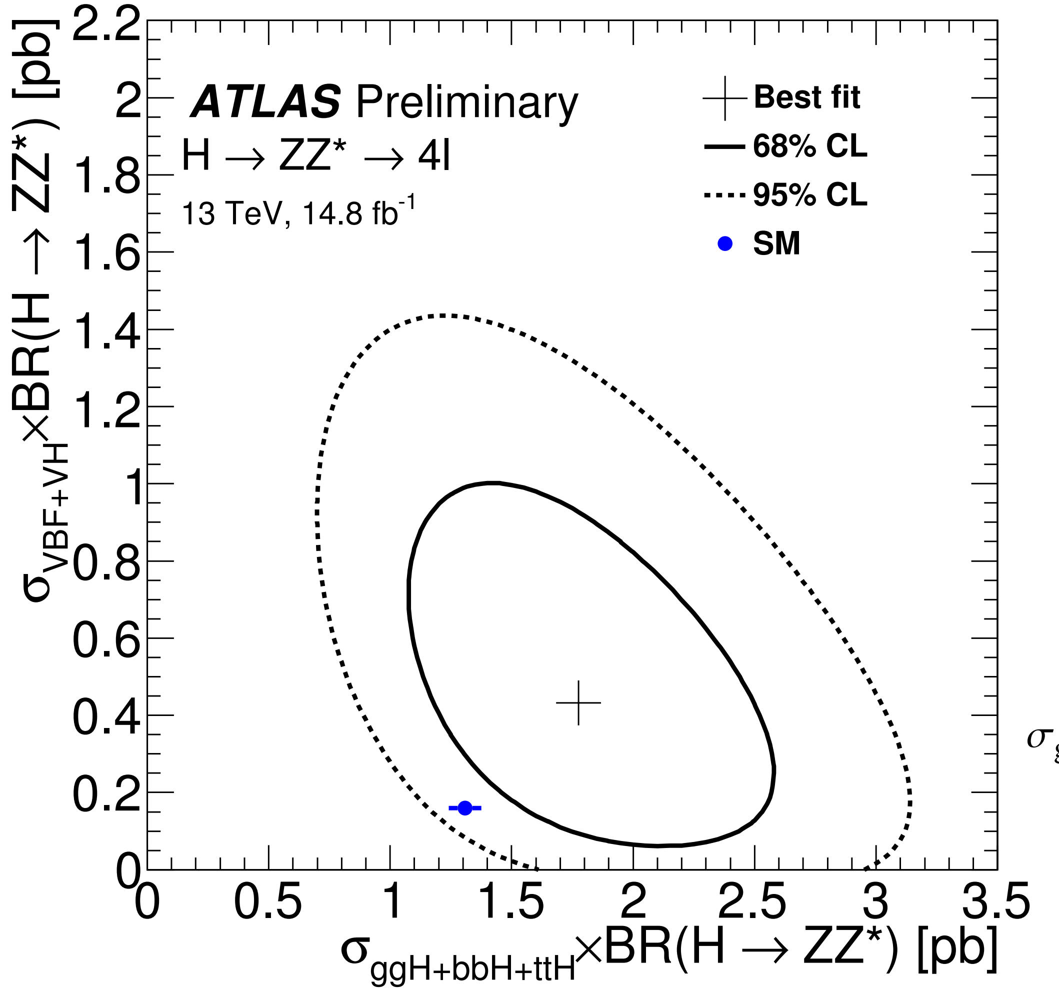

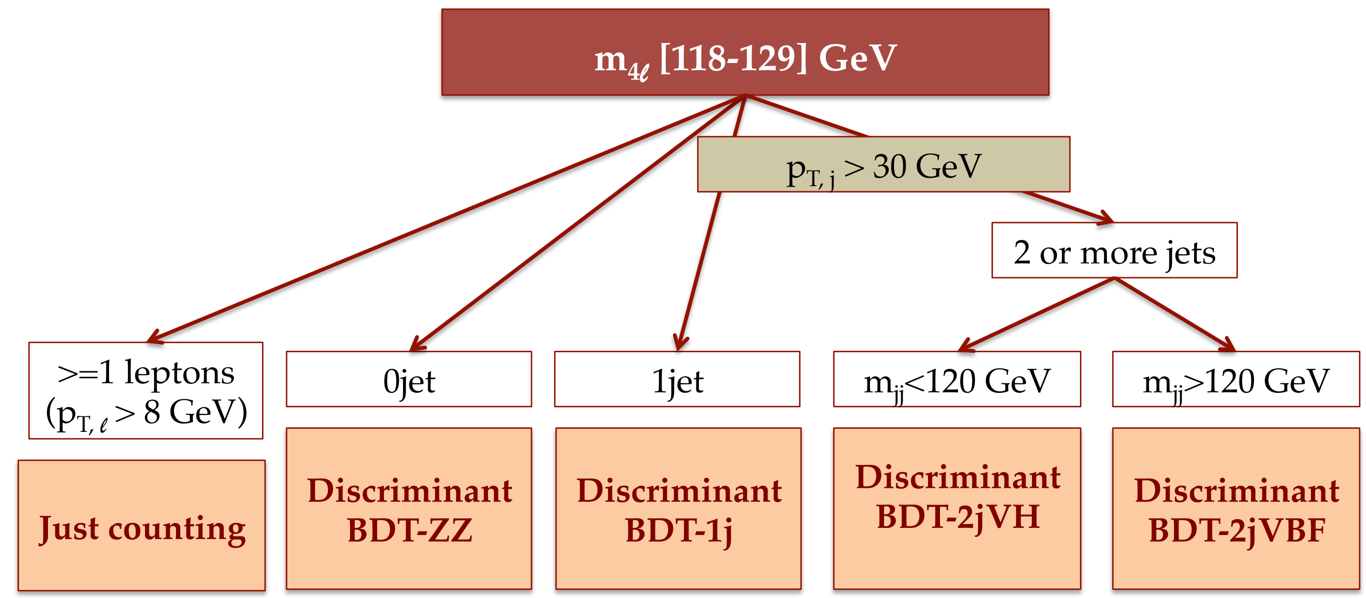

$$\sigma_{ggF+b\bar{b}H+t\bar{t}H} \cdot \mathcal{B}(H \to ZZ^*) = 1.80^{+0.49}_{-0.44} \text{ pb}$$
$$\sigma_{VBF} \cdot \mathcal{B}(H \to ZZ^*) = 0.37^{+0.28}_{-0.21} \text{ pb}$$
$$\sigma_{VH} \cdot \mathcal{B}(H \to ZZ^*) = 0^{+0.15} \text{ pb}$$

$$\sigma_{SM,ggF+b\bar{b}H+t\bar{t}H} \cdot \mathcal{B}(H \to ZZ^*) = 1.31 \pm 0.07 \text{ pb}$$
$$\sigma_{SM,VBF} \cdot \mathcal{B}(H \to ZZ^*) = 0.100 \pm 0.003 \text{ pb}$$
$$\sigma_{SM,VH} \cdot \mathcal{B}(H \to ZZ^*) = 0.059 \pm 0.002 \text{ pb}$$

Compatibility to the **SM prediction**
$\sigma_{ggF+bbH+ttH} \cdot$ B(H → ZZ*) is 1.1σ and $\sigma_{VBF} \cdot$ B(H → ZZ*) is 1.4σ.

- Events in the 118<$m_{4\ell}$<129 GeV range are sorted into exclusive categories.
  - Except in VH-leptonic, a BDT is used to enhance sensitivity.
- Signal obtained from a likelihood fit to the BDT output.
  - The cross-section is then obtained assuming m_H=125.09 GeV.

Summary and Conclusions

- The Higgs is rediscovered at $\sqrt{s}$=13 TeV!
- Utilizing the 4ℓ decay channel, a number of measurements of Higgs properties are made with the new 13 TeV dataset.
    - No significant deviations from the SM are observed.
- Since ICHEP 2016, our 13 TeV dataset has more than doubled.
    - New, more precise tests of the SM are on the way.

Backup

Signal Strength and Total Cross-Section

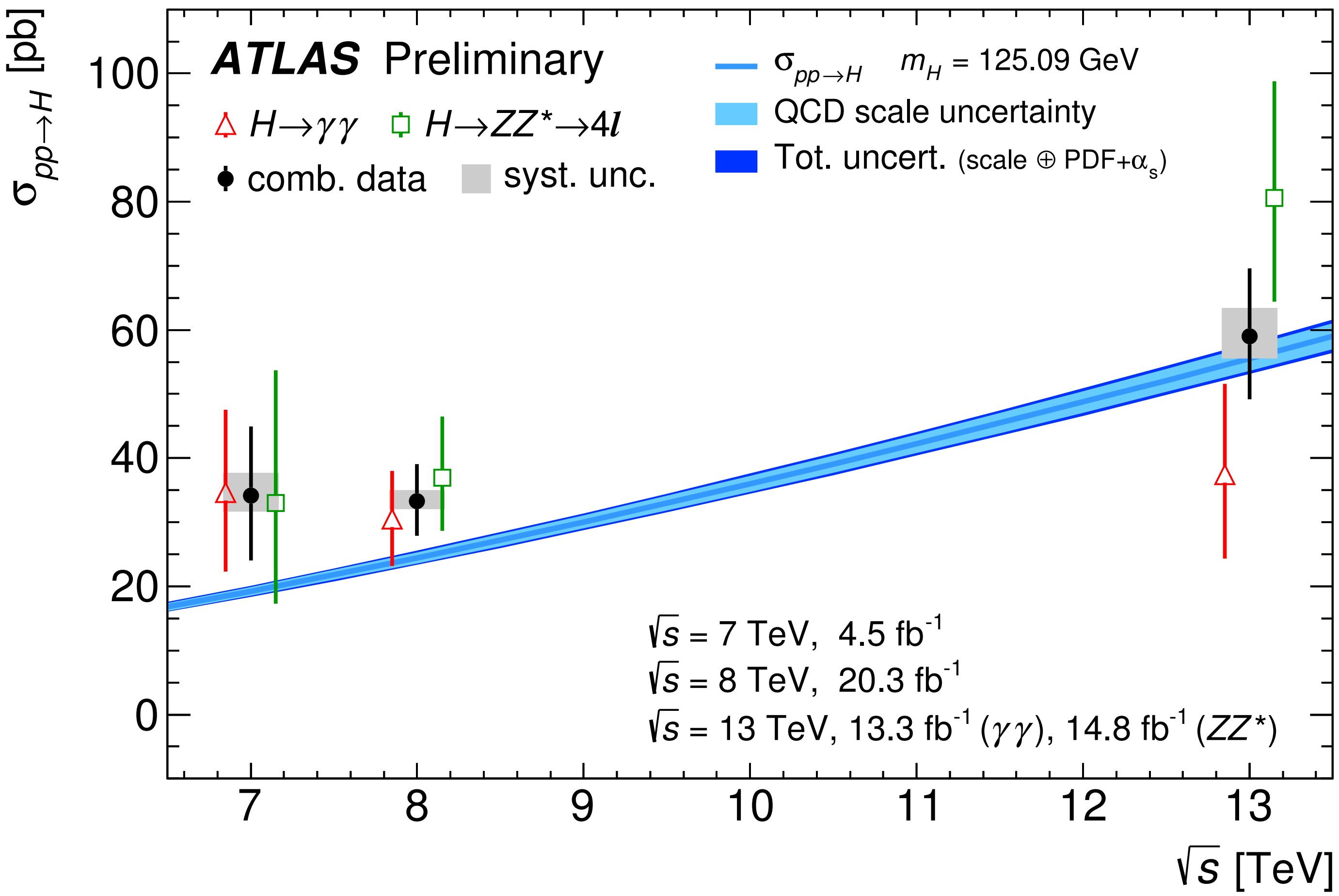

$$\mu = 1.13\,^{+0.18}_{-0.17}$$

No deviations from the SM prediction are observed in the total cross-section or global signal strength.

BSM Sensitivity

JHEP 11 (2013) 043

$$\begin{aligned}
\mathcal{L}_0^V = \Bigg\{ & c_\alpha \kappa_{\rm SM} \left[\frac{1}{2} g_{HZZ}\, Z_\mu Z^\mu + g_{HWW}\, W_\mu^+ W^{-\mu} \right] \\
& - \frac{1}{4} \left[c_\alpha \kappa_{H\gamma\gamma} g_{H\gamma\gamma}\, A_{\mu\nu} A^{\mu\nu} + s_\alpha \kappa_{A\gamma\gamma} g_{A\gamma\gamma}\, A_{\mu\nu} \widetilde{A}^{\mu\nu} \right] \\
& - \frac{1}{2} \left[c_\alpha \kappa_{HZ\gamma} g_{HZ\gamma}\, Z_{\mu\nu} A^{\mu\nu} + s_\alpha \kappa_{AZ\gamma} g_{AZ\gamma}\, Z_{\mu\nu} \widetilde{A}^{\mu\nu} \right] \\
& - \frac{1}{4} \left[c_\alpha \kappa_{Hgg} g_{Hgg}\, G^a_{\mu\nu} G^{a,\mu\nu} + s_\alpha \kappa_{Agg} g_{Agg}\, G^a_{\mu\nu} \widetilde{G}^{a,\mu\nu} \right] \\
& \boxed{- \frac{1}{4} \frac{1}{\Lambda} \left[c_\alpha \kappa_{HZZ}\, Z_{\mu\nu} Z^{\mu\nu} + s_\alpha \kappa_{AZZ}\, Z_{\mu\nu} \widetilde{Z}^{\mu\nu} \right] - \frac{1}{2} \frac{1}{\Lambda} \left[c_\alpha \kappa_{HWW}\, W^+_{\mu\nu} W^{-\mu\nu} + s_\alpha \kappa_{AWW}\, W^+_{\mu\nu} \widetilde{W}^{-\mu\nu} \right]} \\
& - \frac{1}{\Lambda} c_\alpha \left[\kappa_{H\partial\gamma}\, Z_\nu \partial_\mu A^{\mu\nu} + \kappa_{H\partial Z}\, Z_\nu \partial_\mu Z^{\mu\nu} + \left(\kappa_{H\partial W}\, W_\nu^+ \partial_\mu W^{-\mu\nu} + h.c. \right) \right] \Bigg\} X_0
\end{aligned}$$

- Madgraph5_aMC@NLO is used to generate template samples.
- Then the morphing technique is used to obtain predictions for any value of the BSM couplings.

- Exclusive event category yields are also used to probe for BSM interactions.
- BSM effects are parameterized using the Higgs characterization model
  - BSM couplings k_{HVV} (scalar) and k_{AVV} (pseudo-scalar) are studied (assuming cos(α)=1 and the couplings are the same for W and Z).
  - VBF and VH production yields scale with k_{BSM}^4.

BSM Sensitivity

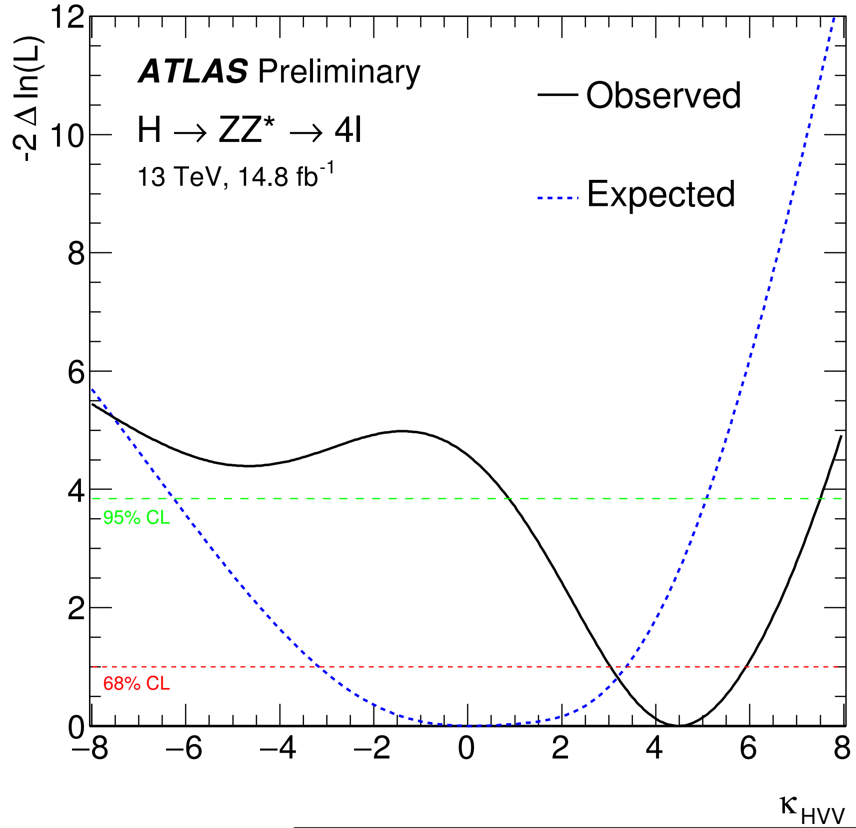

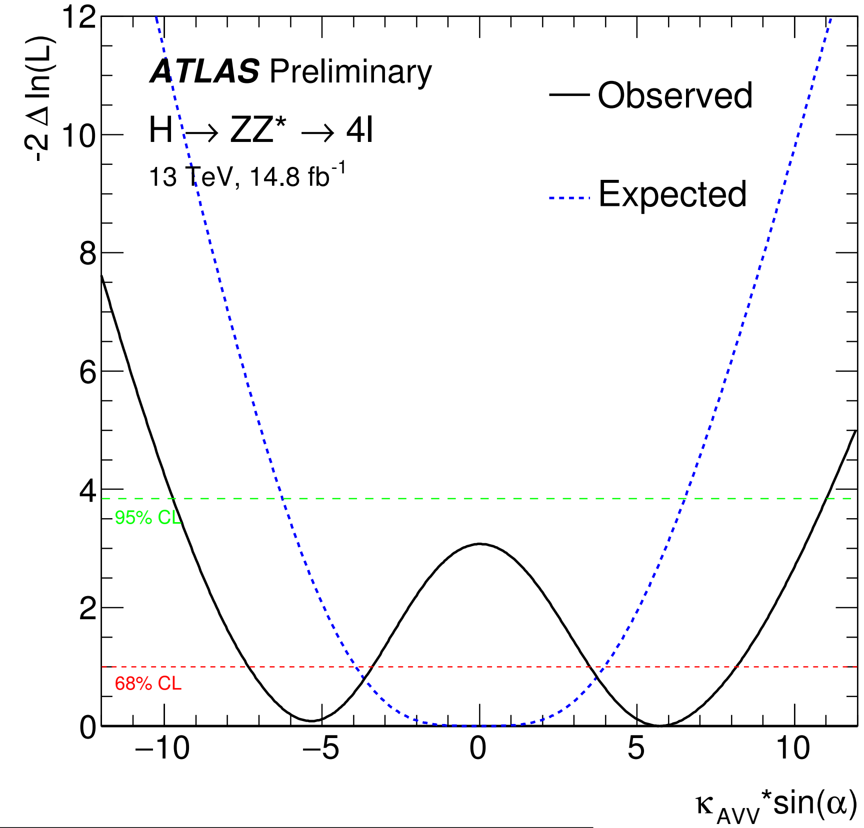

Not excluded range at 95% CL	κ_{HVV}		$\kappa_{AVV} \cdot \sin\alpha$	
	expected	observed	expected	observed
	$[-6.3, 5.1]$	$[0.9, 7.5]$	$[-6.3, 6.5]$	$[-9.7, 11.0]$

- Limits are derived from a fit to the yields (no kinematic information is used), considering one coupling at a time.
  - ggF production is fixed to the SM value for the fit.
- Limits are weaker than SM expectation.
  - k_{HVV} is 2.1σ compatible with 0 and k_{AVV} 1.8σ.

H->γγ

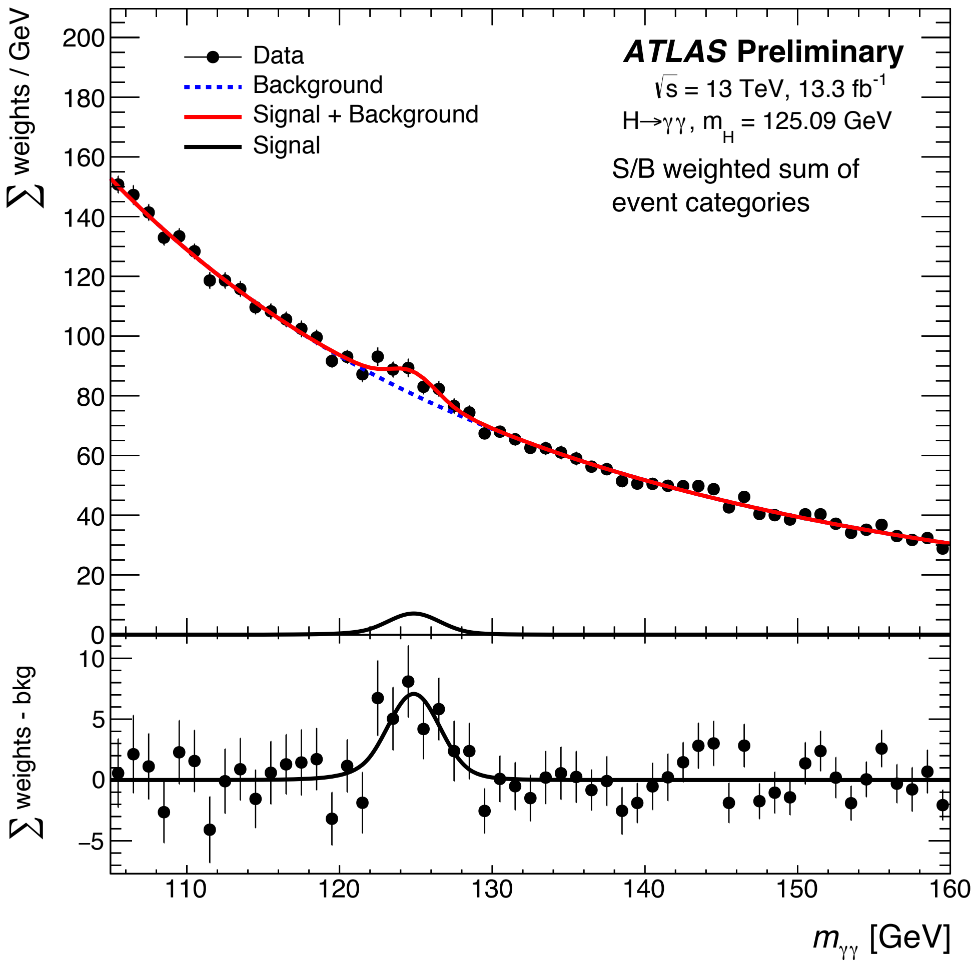

- Events are split into 13 different exclusive categories, based on
  - Production modes
  - Decay products of particles produced with the Higgs
- The fiducial measurement uses the inclusive distribution instead.
- Background shape is parametrized in each category from MC, and fit to data.
- Signal is extracted from a simultaneous fit to the $m_{\gamma\gamma}$ distribution across all categories.

Combined γγ-4ℓ Results

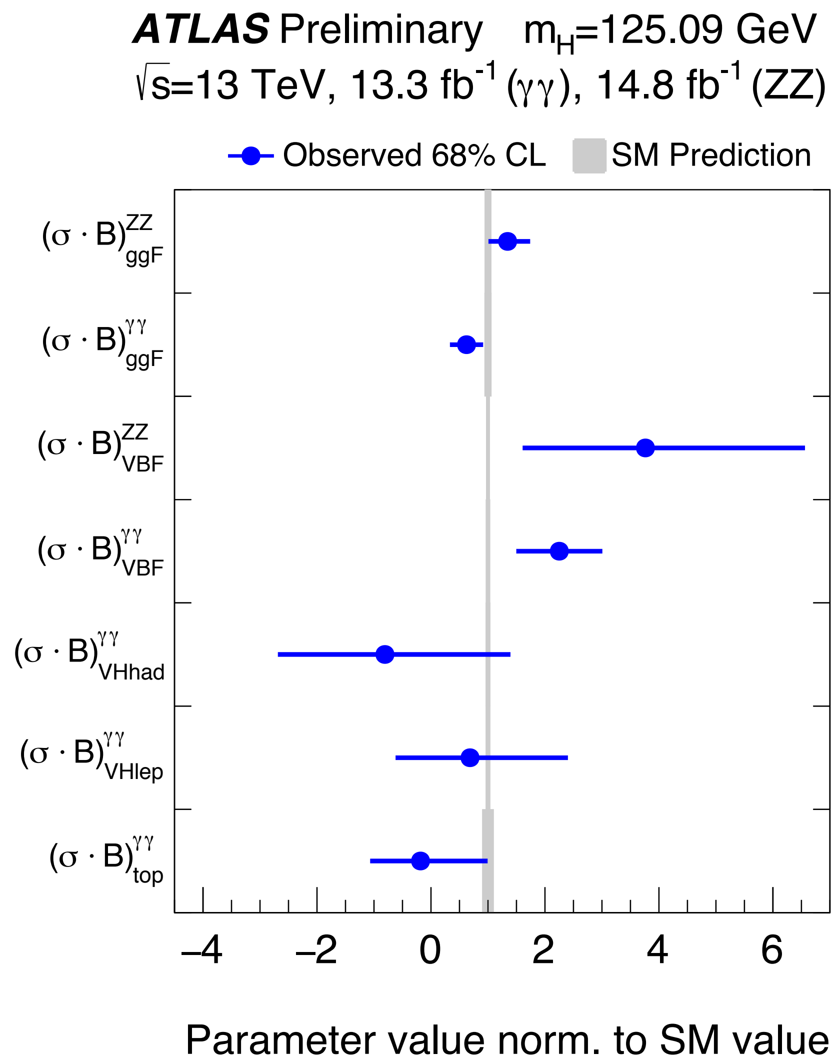

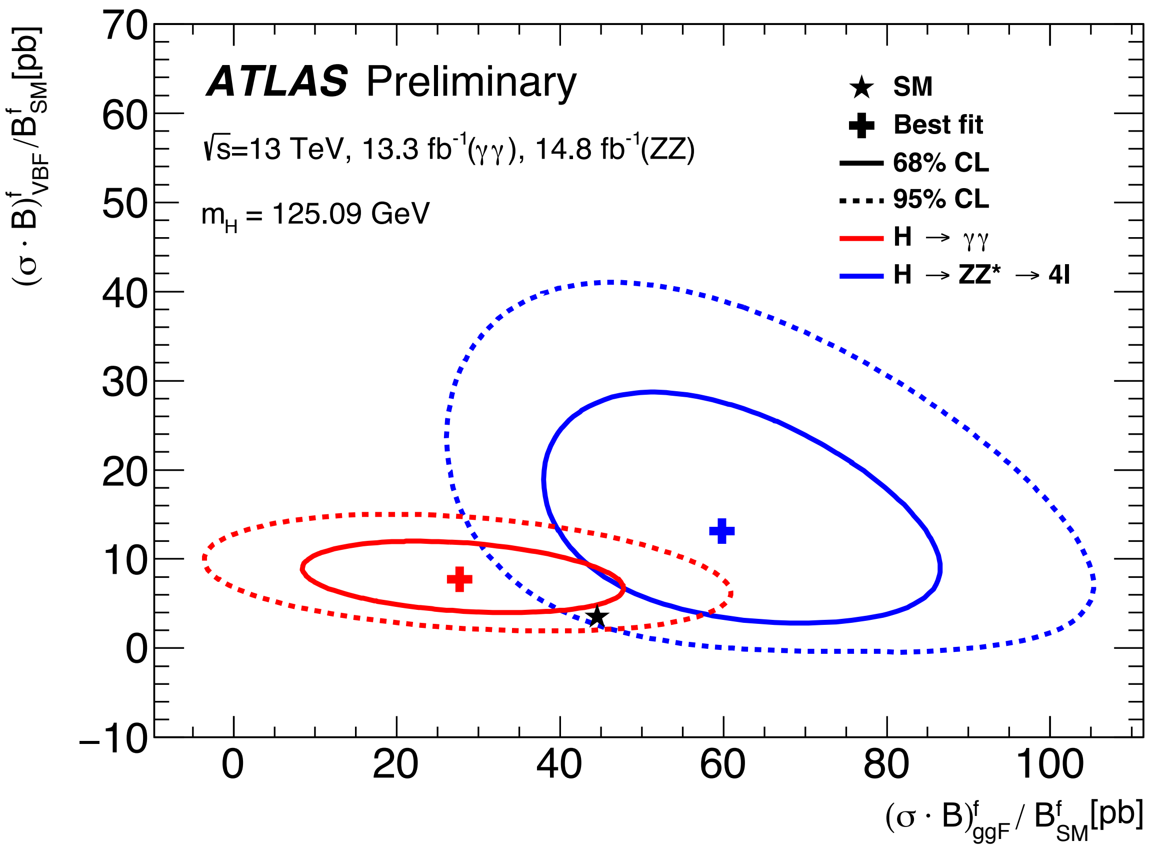

- Each σ_ixBR^f parameter is treated as independent in the fit: results are shown upper left.
- Upper right plot shows the fit result divided by the SM BR.

Combined Cross-section Results

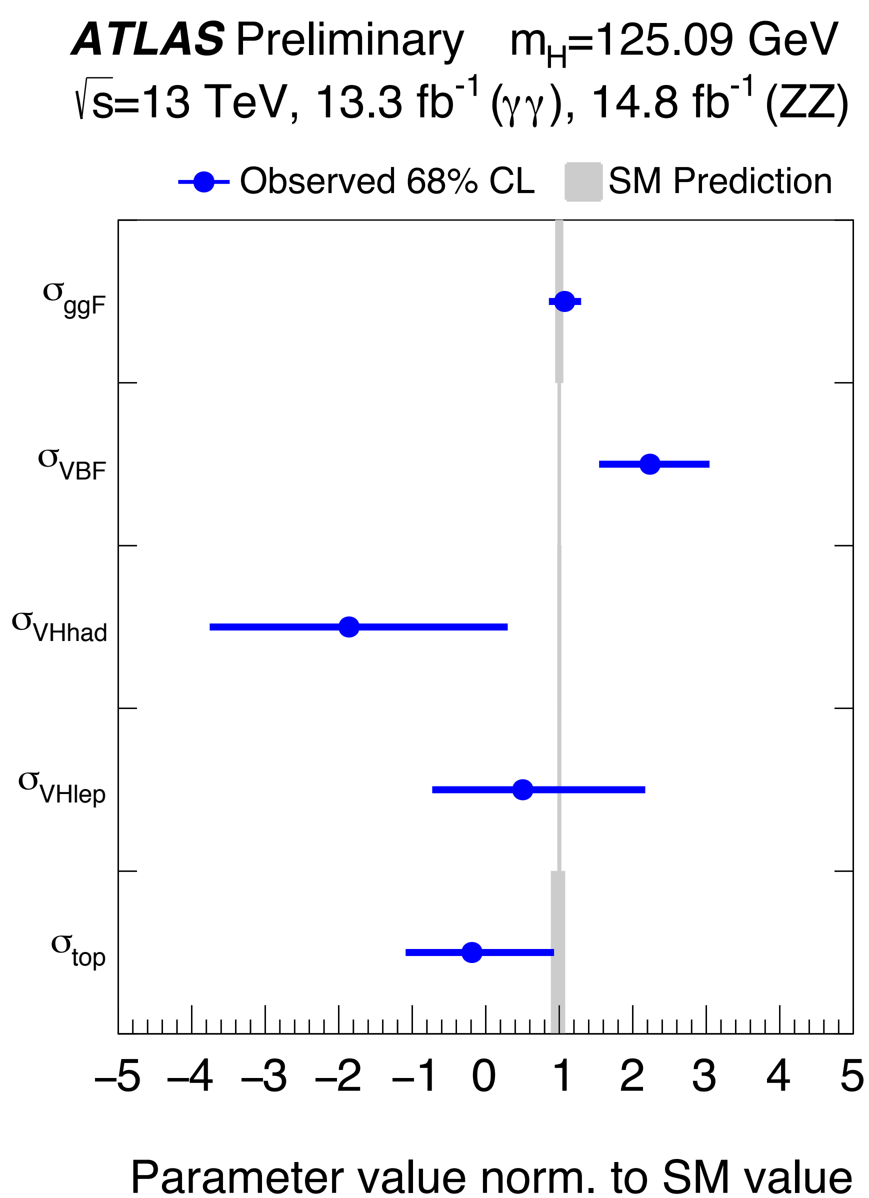

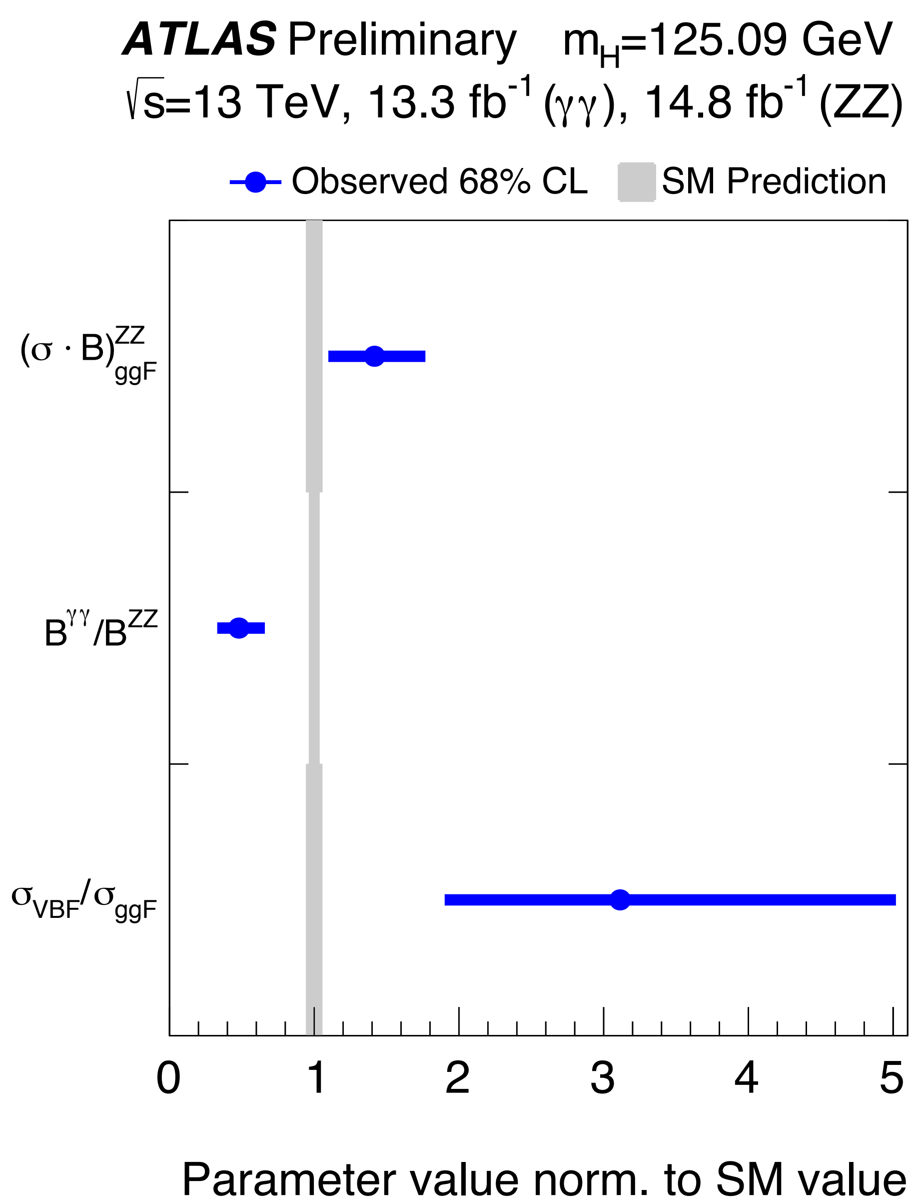

- Left: BRs are assumed to take their SM values.
- Right: the σ_ixBR^f values are parameterized in terms of the ratios σ_i/σ_{ggF} and BR^f/BR^{ZZ}.
- All results are consistent with SM expectations.

4ℓ Event Selection

Physics Objects	
Electrons	
Loose Likelihood quality electrons with hit in innermost layer, $E_T > 7$ GeV and $|\eta| < 2.47$	
Muons	
Loose identification	
Calo-tagged muons with $p_T > 15$ GeV and $|\eta| < 0.1$	
Combined, stand-alone (with ID hits if available) and segment tagged muons with $p_T > 5$ GeV	
Jets	
anti-k_T jets with $p_T > 30$ GeV, $|\eta| < 4.5$ and passing pile-up jet rejection requirements	
Event Selection	
Quadruplet Selection	Require at least one quadruplet of leptons consisting of two pairs of same-flavour opposite-charge leptons fulfilling the following requirements: p_T thresholds for three leading leptons in the quadruplet - 20, 15 and 10 GeV Maximum one calo-tagged or standalone muon per quadruplet Select best quadruplet to be the one with the (sub)leading dilepton mass (second) closest the Z mass Leading di-lepton mass requirement: 50 GeV $< m_{12} <$ 106 GeV Sub-leading di-lepton mass requirement: $12 < m_{34} < 115$ GeV Remove quadruplet if alternative same-flavour opposite-charge di-lepton gives $m_{\ell\ell} < 5$ GeV $\Delta R(\ell, \ell') > 0.10$ (0.20) for all same (different) flavour leptons in the quadruplet
Isolation	Contribution from the other leptons of the quadruplet is subtracted Muon track isolation ($\Delta R <= 0.30$): $\Sigma p_T/p_T < 0.15$ Muon calorimeter isolation ($\Delta R <= 0.20$): $\Sigma E_T/p_T < 0.30$ Electron track isolation ($\Delta R <= 0.20$) : $\Sigma E_T/E_T < 0.15$ Electron calorimeter isolation ($\Delta R <= 0.20$) : $\Sigma E_T/E_T < 0.20$
Impact Parameter Significance	Apply impact parameter significance cut to all leptons of the quadruplet. For electrons : $d_0/\sigma_{d_0} < 5$ For muons : $d_0/\sigma_{d_0} < 3$
Vertex Selection	Require a common vertex for the leptons χ^2/ndof < 6 for 4μ and < 9 for others.

Electron and Muon Performance

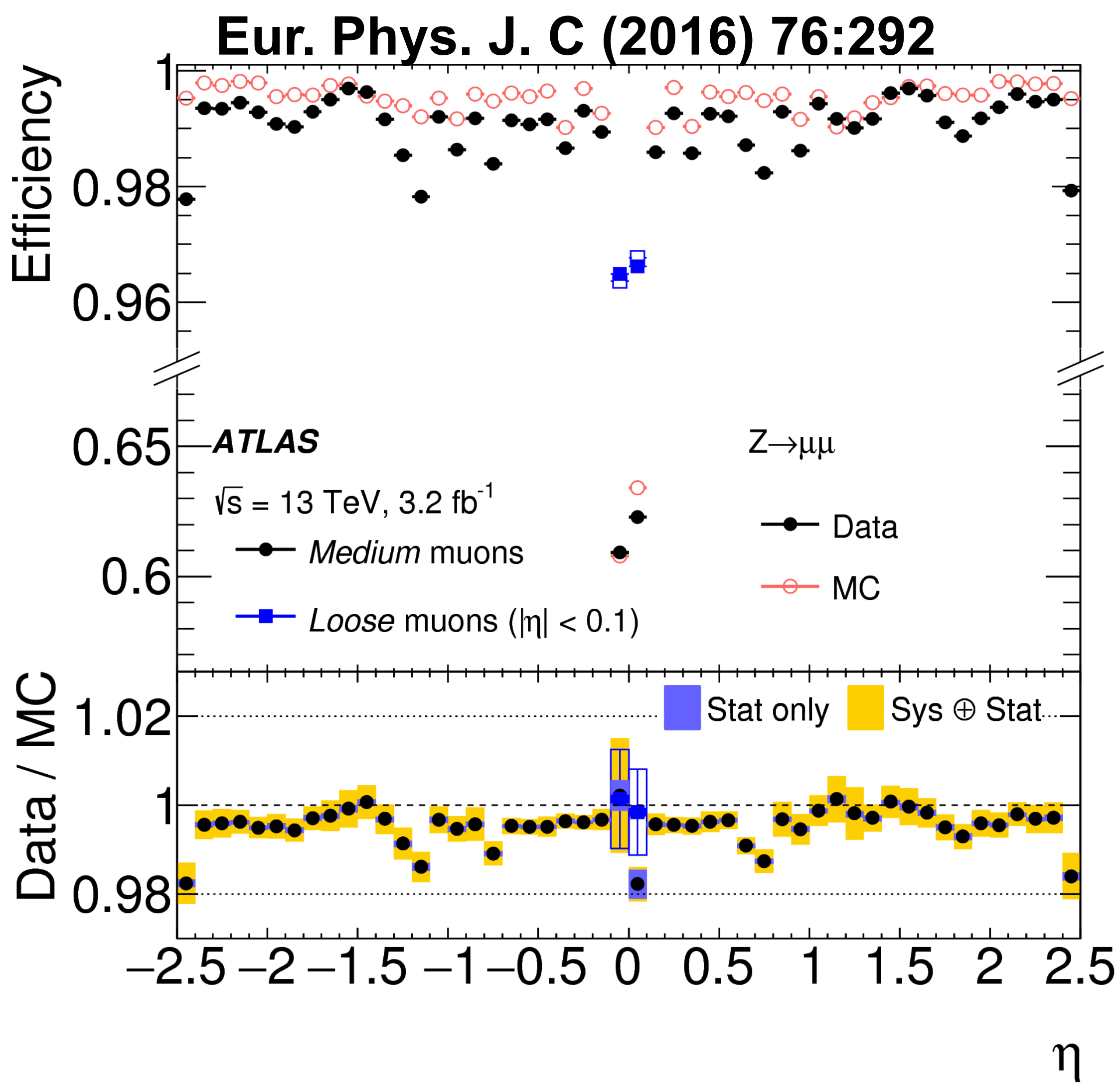

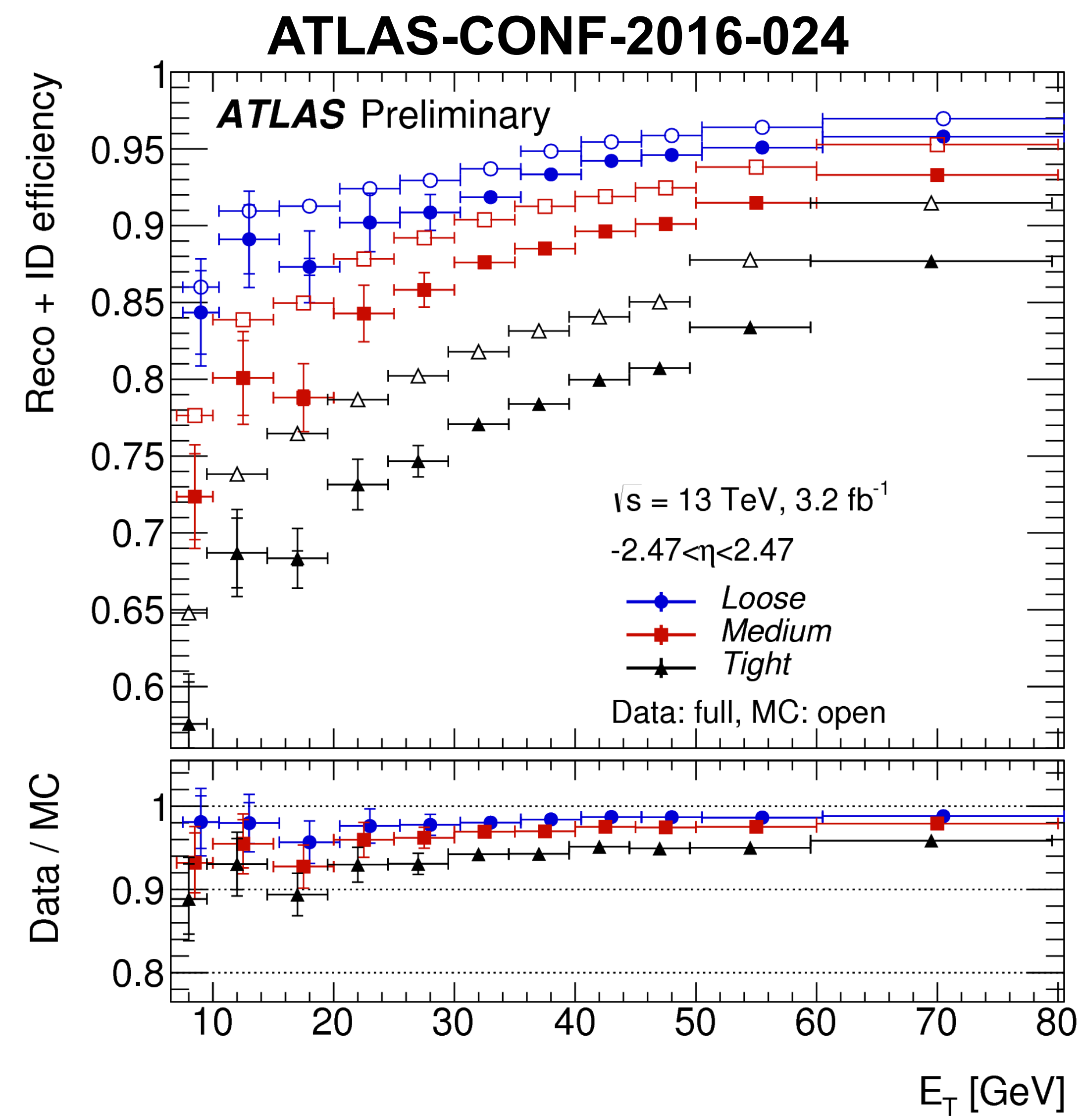

Detector performance well understood, data used to correct simulation.

$m_{4\ell}$ distributions per channel

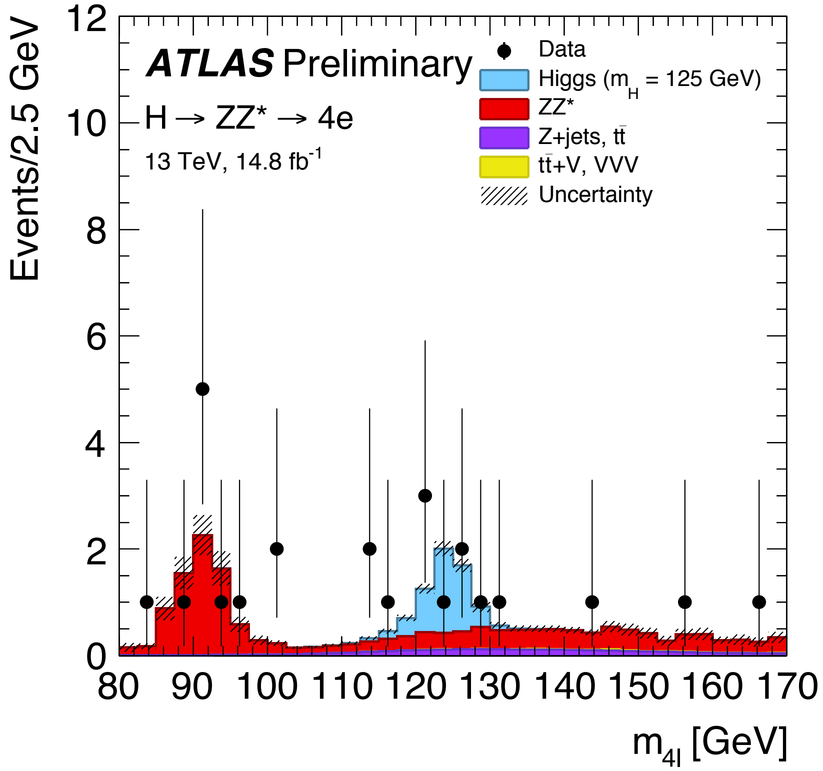

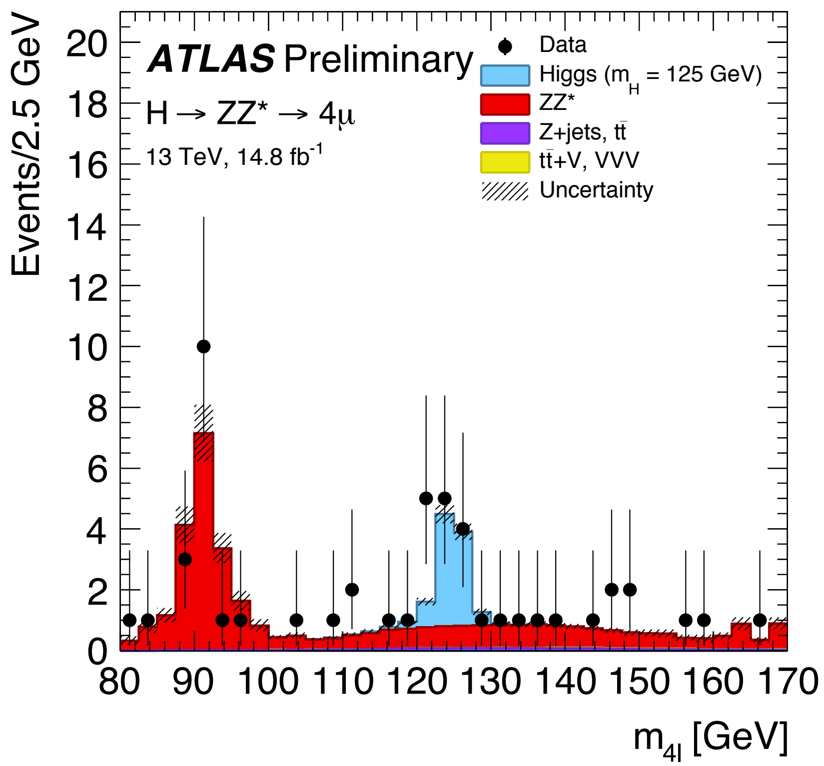

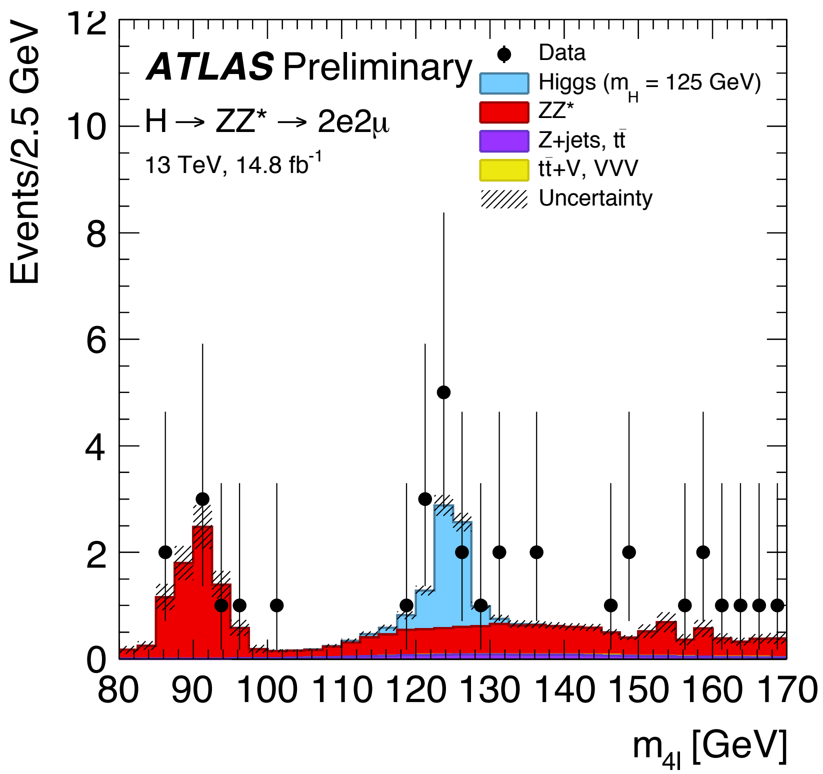

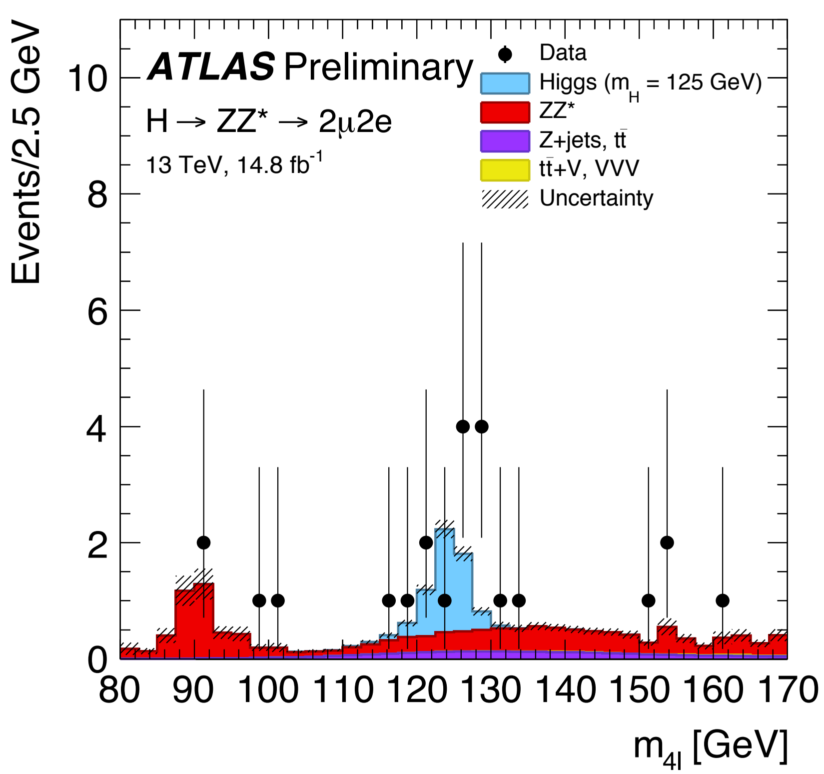

$m_{4\ell}$ distributions per channel (BDT_{ZZ}>0)

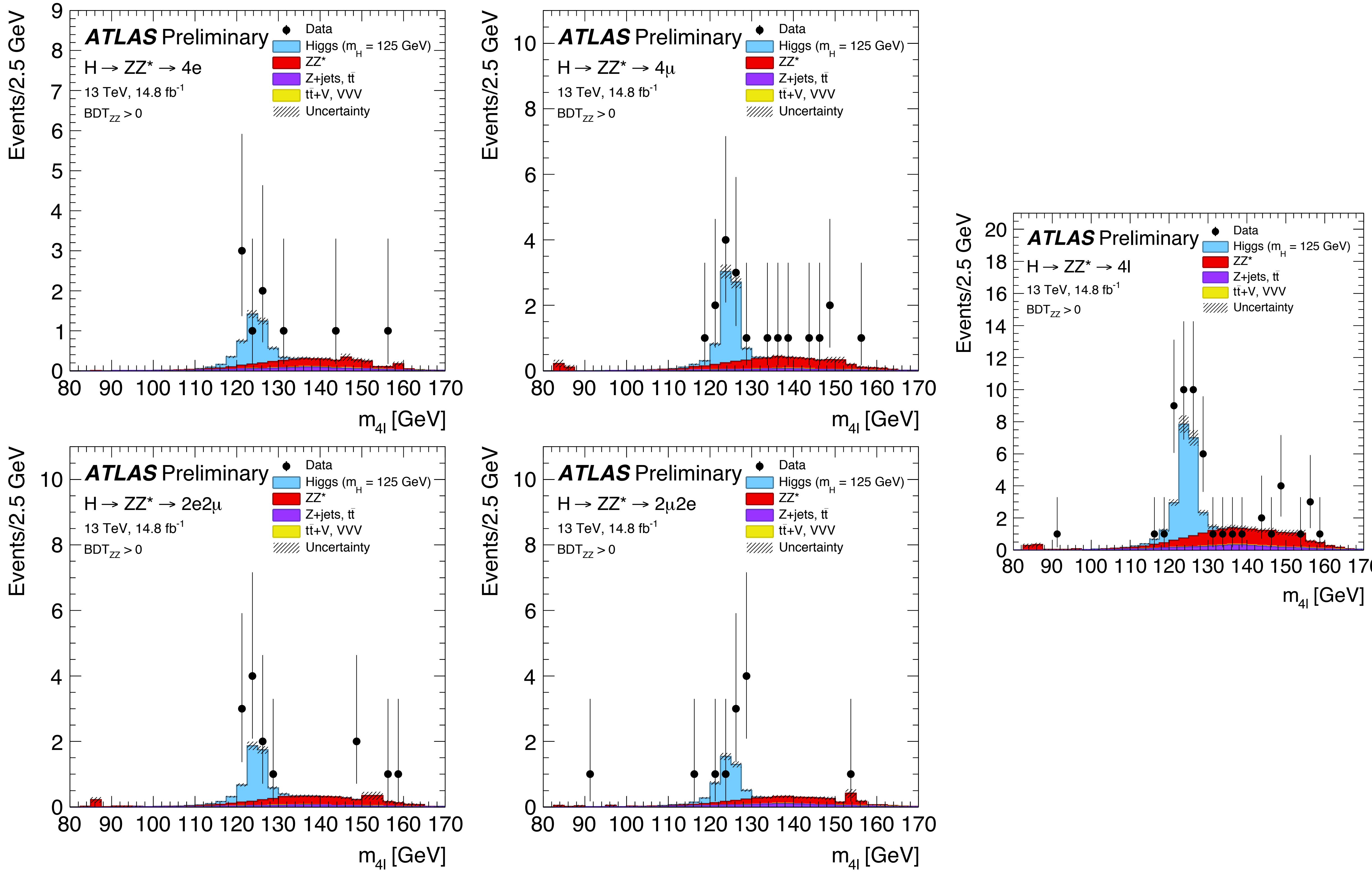

Fiducial Volume

Lepton definition	
Muons: $p_T > 5$ GeV, $\lvert\eta\rvert < 2.7$	Electrons: $p_T > 7$ GeV, $\lvert\eta\rvert < 2.47$
Pairing	
Leading pair:	SFOS lepton pair with smallest $\lvert m_Z - m_{\ell\ell}\rvert$
Sub-leading pair:	Remaining SFOS lepton pair with smallest $\lvert m_Z - m_{\ell\ell}\rvert$
Event selection	
Lepton kinematics:	Leading lepton $p_T > 20, 15, 10$ GeV
Mass requirements:	$50 < m_{12} < 106$ GeV; $12 < m_{34} < 115$ GeV
Lepton separation:	$\Delta R(\ell_i, \ell_j) > 0.1(0.2)$ for same (opposite) flavor leptons
J/ψ veto:	$m(\ell_i, \ell_j) > 5$ GeV for all SFOS lepton pairs
Mass window:	$115 < m_{4\ell} < 130$ GeV

$$N_{Data}(m_{4\ell})_i = \mathcal{L}_{\text{int}} \cdot \sigma^{\text{tot}} \cdot \mathcal{B}(H \to 4\ell) \cdot$$
$$\Big(f_i \cdot PDF(m_{4\ell})_{sig,i} \cdot \sum_{proc}(r_{\text{proc}} \cdot \mathcal{A}_{\text{proc},i} \cdot C_{\text{proc},i}) + PDF(m_{4\ell})_{bkg,i} \cdot N_{bkg,i}\Big).$$

Acceptance factors $\mathcal{A}$[%]					
Decay	Production mode				
Channel	ggF	VBF	WH	ZH	$t\bar{t}H$
4μ	50.9	55.0	43.8	46.5	53.6
$4e$	39.6	43.9	34.4	36.0	44.6
$2\mu 2e$	40.0	42.9	34.0	35.5	42.4
$2e2\mu$	45.9	48.6	38.0	40.4	47.2

Correction factors C[%]					
Decay	Production mode				
Channel	ggF	VBF	WH	ZH	$t\bar{t}H$
4μ	62.6	64.2	60.8	60.5	41.8
$4e$	42.1	43.2	43.0	42.7	38.7
$2\mu 2e$	46.9	50.9	49.1	48.6	41.7
$2e2\mu$	53.1	54.7	51.8	50.2	36.7

Exclusive Categories Yields

Table 12: The expected and observed yields in the 0-jet, 1-jet, 2-jet with $m_{jj} > 120$ GeV (*VBF-enriched*), 2-jet with $m_{jj} < 120$ GeV (*VH-enriched*) and VH-leptonic categories. The yields are given for the different production modes, assuming $m_H = 125$ GeV, the ZZ^* and reducible background for 14.8 fb^{-1} at $\sqrt{s} = 13$ TeV. The estimates are given for the $m_{4\ell}$ mass range 118–129 GeV. Full uncertainties are provided.

Analysis	Signal				Background		Total	Observed
category	ggF + $b\bar{b}H$ + $t\bar{t}H$	VBF	WH	ZH	ZZ^*	Z + jets, $t\bar{t}$	expected	
0-jet	11.2 ± 1.4	0.120 ± 0.019	0.047 ± 0.007	0.060 ± 0.006	6.2 ± 0.6	0.84 ± 0.12	18.4 ± 1.6	21
1-jet	5.7 ± 2.4	0.59 ± 0.05	0.137 ± 0.012	0.091 ± 0.008	1.62 ± 0.21	0.44 ± 0.07	8.5 ± 2.4	12
2-jet VBF enriched	1.9 ± 0.9	0.92 ± 0.07	0.074 ± 0.007	0.052 ± 0.005	0.22 ± 0.05	0.24 ± 0.11	3.4 ± 0.9	9
2-jet VH enriched	1.1 ± 0.5	0.084 ± 0.009	0.143 ± 0.012	0.101 ± 0.009	0.166 ± 0.035	0.088 ± 0.011	1.6 ± 0.5	2
VH-leptonic	0.055 ± 0.004	< 0.01	0.067 ± 0.004	0.011 ± 0.001	0.016 ± 0.002	0.012 ± 0.010	0.16 ± 0.01	0
Total	20 ± 4	1.71 ± 0.14	0.47 ± 0.04	0.315 ± 0.027	8.2 ± 0.9	1.62 ± 0.07	32 ± 4	44

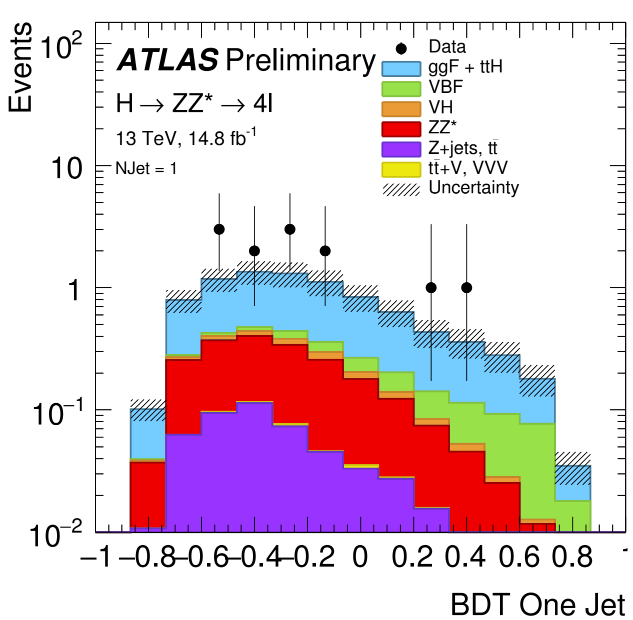

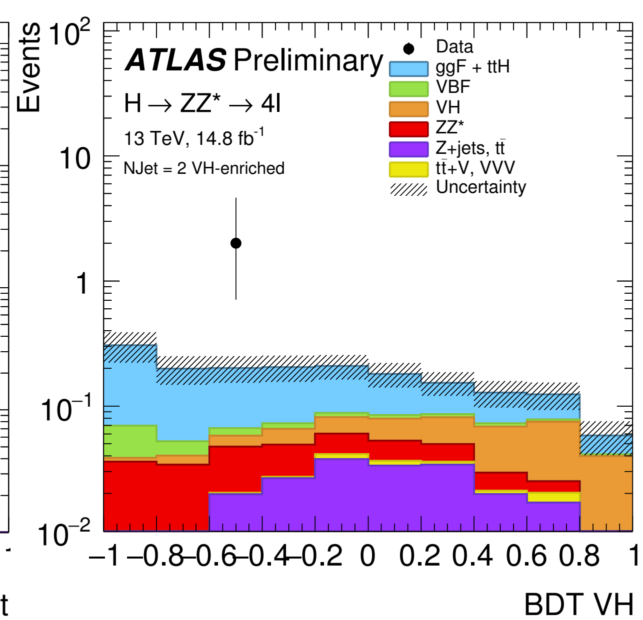

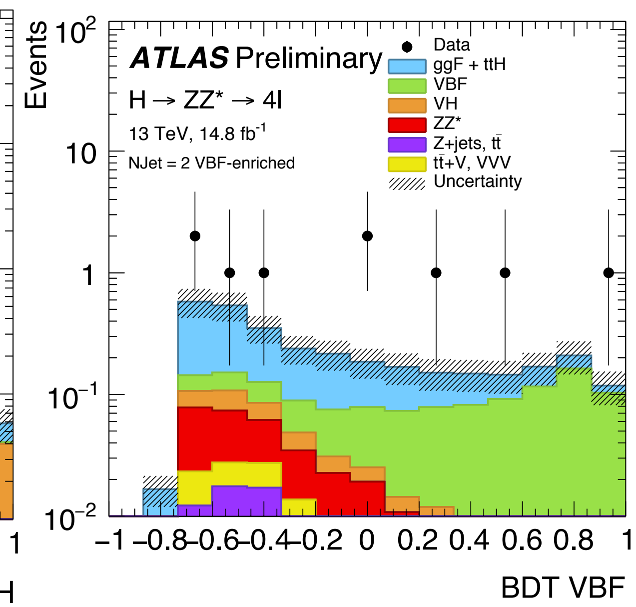

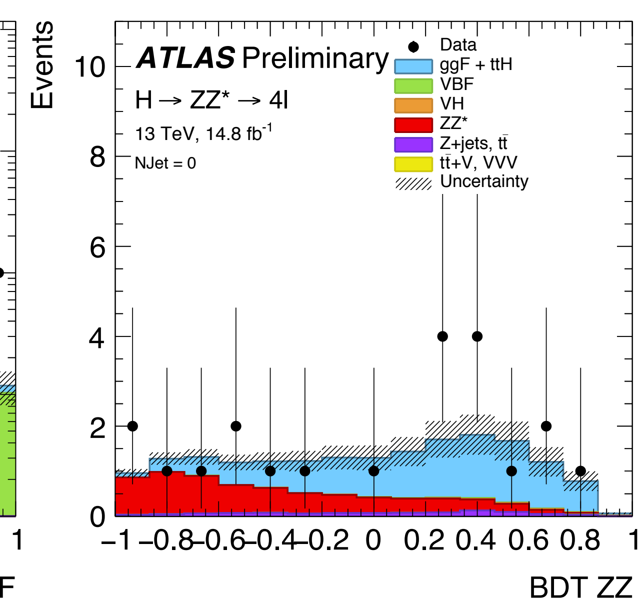

DESY Group Efforts

- Focused on the H->4ℓ differential cross-section measurement on a ~Moriond timescale.
- Two main efforts:
  - Reducible background shapes, for both muon and electron backgrounds.
  - Unfolding validation: compare the current bin-by-bin unfolding method used in the analysis to other methods to evaluate possible biases.
  - Manpower: Sarah, me.

Reducible Background Shapes

- The differential cross-section analysis will use the variables $p_{T,4\ell}$ (inclusive, in the 0-jet region, and in the 1-jet region), $y_{4\ell}$, n_{jet}, m_{12}, m_{34}, m_{12} vs. m_{34}, $\cos(\Theta^*)$, and leading jet p_T.
- Reducible background from Z+jets and tt is a relatively small effect but needs to be modeled.

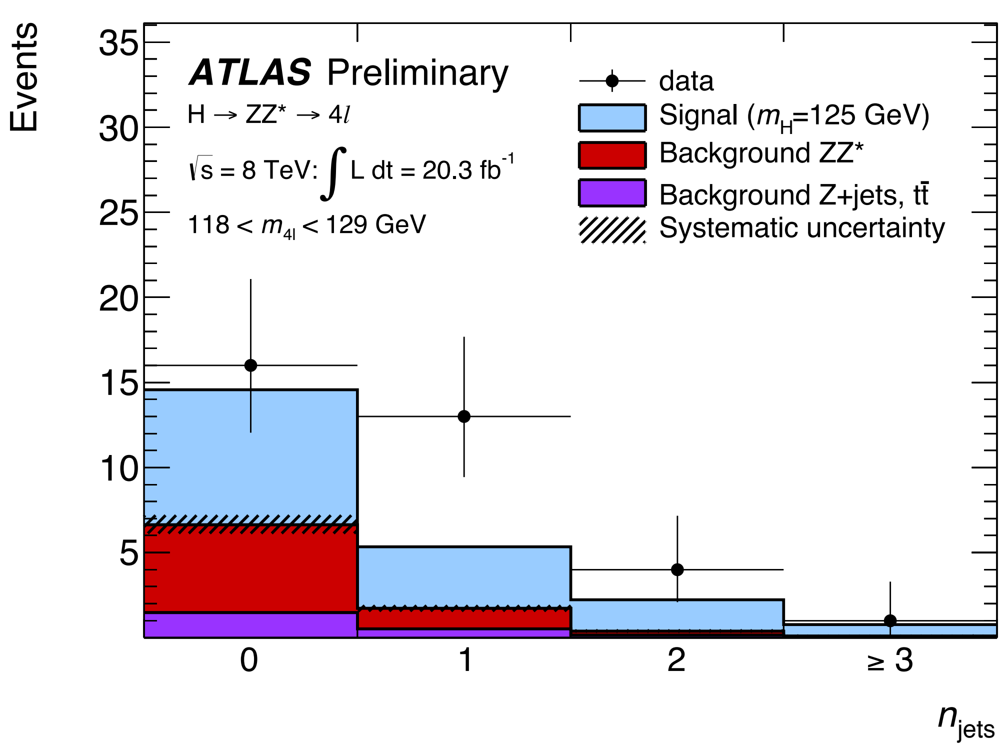

ICHEP luminosity